Supporting Information

# Preparation of Phosphine Oxides with Anthrylphenyl, Pyrenylphenyl, Anthrylethynyl, and Pyrenylethynyl Groups: Luminescent Properties and Conformational Polymorphs

Ryunosuke Konno, Manami Fujita, Rima Maekawa, Hyuma Masu,
and Kosuke Katagiri*

**General.** All commercially available reagents were used without further purification. $^{1}$H, $^{13}$C and $^{31}$P NMR spectra were recorded on an Agilent UNITY INOVA 500 spectrometers (500 MHz for $^{1}$H, 126 MHz for $^{13}$C, and 200 MHz for $^{31}$P). Mass spectral data were obtained using a JEOL JMS-T100LP mass spectrometer in the positive-ion detection mode. Ultraviolet-visible (UV-vis) spectra were recorded using a JASCO model V650 spectrophotometer. Fluorescence spectra were recorded using a JASCO FP8050 spectrophotometer (in solution) and JASCO FP8600 (in solid).

**Synthesis.**

Scheme S1. Synthesis of [4-(9-anthryl)phenyl]diphenylphosphine oxide **1**.

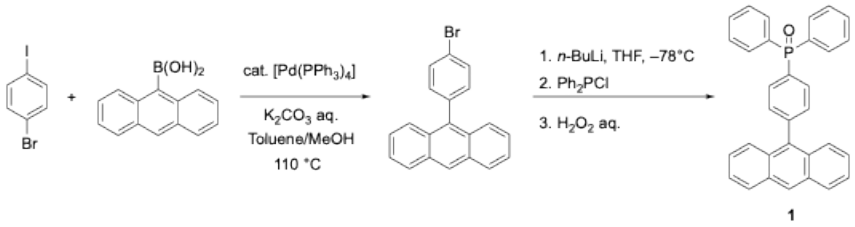


1

Scheme S2. Synthesis of [4-(1-pyrenyl)phenyl]diphenylphosphine oxide **3**.

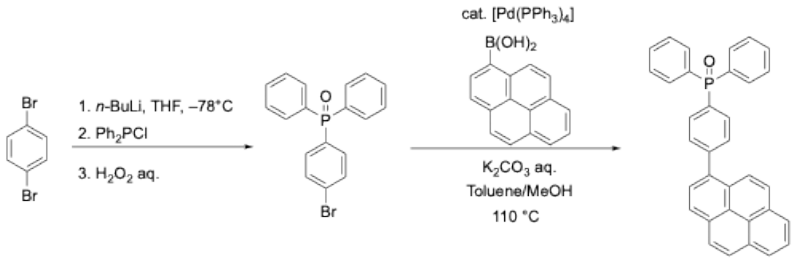


3

Scheme S3. Synthesis of [4-(9-anthryl)ethynyl]diphenylphosphine oxide **2** and [4-(1-pyrenyl)ethynyl]diphenylphosphine oxide **4** by route I.

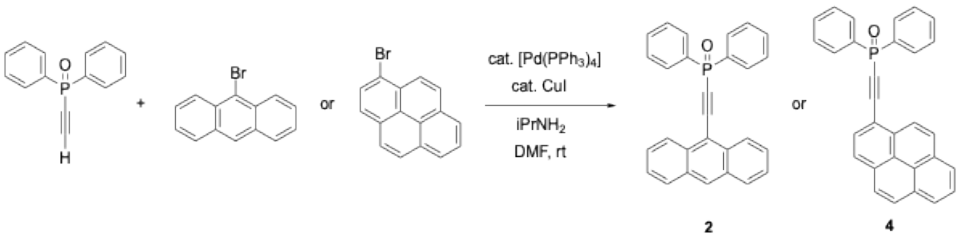


Scheme S4. Synthesis of [4-(9-anthryl)ethynyl]diphenylphosphine oxide **2** and [4-(1-pyrenyl)ethynyl]diphenylphosphine oxide **4** by route II.

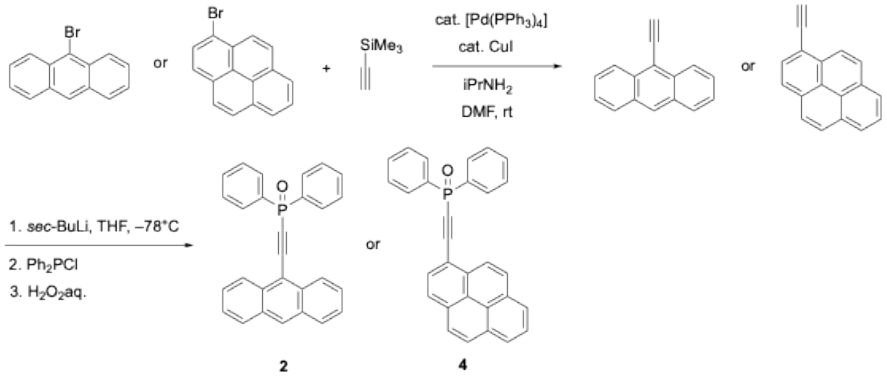


Scheme S5. Synthesis of [4-(9-anthryl)ethynyl]diphenylphosphine oxide **2** and [4-(1-pyrenyl)ethynyl]diphenylphosphine oxide **4** by route III.

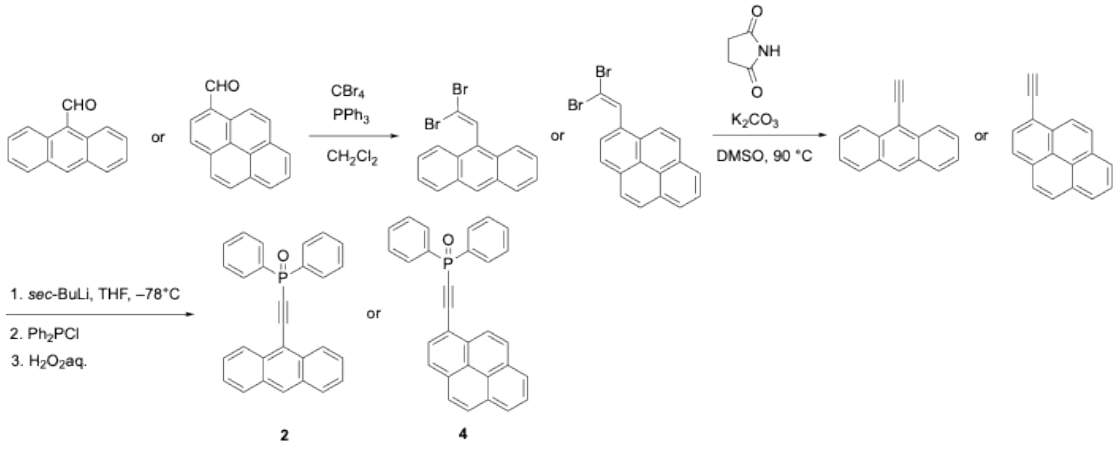

***Synthesis of 9-(4-bromophenyl)anthracene***

A mixture of 1-bromo-4-iodobenzene (0.568 g, 2.01 mmol), 9-anthracene boronic acid (0.671 g, 3.21 mmol), $Pd(PPh_3)_4$ (0.237 g, 0.205 mmol), 2 M $K_2CO_3$ aq. (1.5 mL, 3 mmol) in toluene/MeOH (*v*/*v*= 20 mL/2 mL) was refluxed under $N_2$ at 110°C for overnight. After cooling to room temperature, the mixture was filtrated through Celite, quenched with HCl, extracted with chloroform, and washed with brine. The organic layer was dried over anhydrous $Na_2SO_4$ and evaporated under reduced pressure. Then, the crude product was purified by column chromatography over silica gel using hexane as eluent. Target molecule was obtained as white solid (0.557g, 83.2%).

$^1$H NMR (500 MHz, $CDCl_3$, 25 °C): $\delta$ 8.52 (s, 1H($H^7$)), 8.05 (d, $J$ = 8.5, 2H($H^6$)), 7.72 (d, $J$ = 8.5, 2H($H^3$)), 7.63 (dd, $J$ = 0.5, 8.5 Hz, 2H($H^2$)), 7.47 (td, $J$ = 1.0, 6.5 Hz, 2H($H^5$)), 7.34 (td, $J$ = 1.0, 7.5 Hz, 2H($H^4$)), 7.32 (d, 8.5 Hz, 2H($H^1$)) ppm.

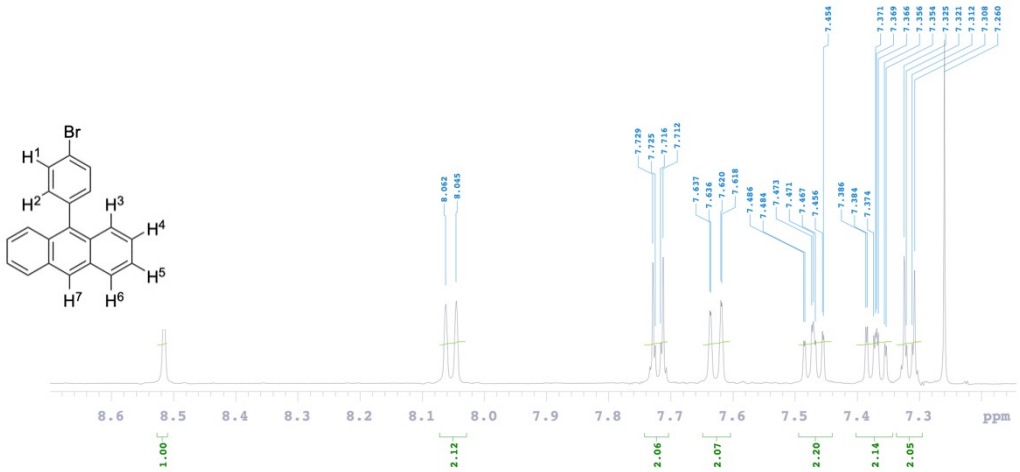


Fig. S1. $^1$H NMR spectrum of 9-(4-Bromophenyl)anthracene in $CDCl_3$.

***Synthesis of [4-(9-anthryl)phenyl]diphenylphosphine oxide 1***

Under a $N_2$ atmosphere, 9-(4-bromophenyl)anthracene (0.359 g, 1.08 mmol) were dissolved in anhydrated tetrahydrofuran (12 mL). The solution was cooled to –78°C and added *n*-BuLi (1.52 M in *n*-hexane, 1.5 mL, 2.3 mmol). After stirred for 30 min, chlorodiphenylphosphine (0.28 mL, 1.5 mmol) was added to mixture and reacted at room temperature for 3 hours. Subsequently, water was incorporated to deactivate any residual *sec*-BuLi, and then hydrogen peroxide (30% , 1 mL) was added and stirred for 30 minutes. After the reaction, the mixture was quenched with water, extracted with chloroform, and washed with brine. The organic layer was dried over anhydrous $Na_2SO_4$ and evaporated under reduced pressure. Then, the crude product was purified by column chromatography

over silica gel using $CHCl_3$, $CHCl_3$/MeOH (3:1 *v*/*v*) as eluent. Compound **1** was obtained White solid (0.244 g, 50.0%).

$^1H$ NMR (500 MHz, $CDCl_3$, 25 °C): $\delta$ 8.53 (s, 1H($H^{10}$)), 8.06 (d, $J$ = 8.5 Hz, 2H($H^9$)), 7.89-7.81 (m, 6H($H^1$, $H^4$)), 7.63-7.54 (m, 10H($H^2$, $H^3$, $H^5$, $H^6$)), 7.48 (t, $J$ = 7, 7.5 Hz, 2H($H^8$)), 7.38 (t, $J$ = 7.5 Hz, 2H($H^7$)) ppm.

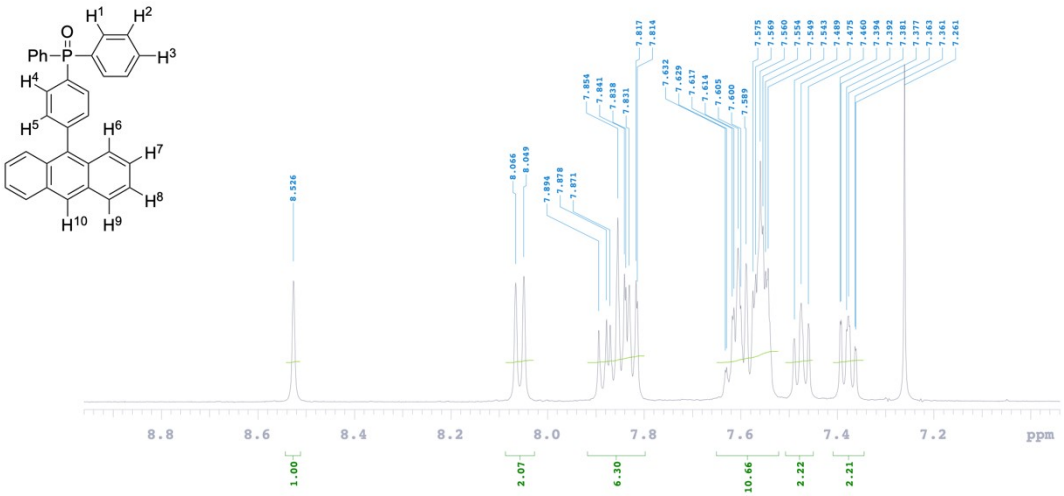


Fig. S2. $^1H$ NMR spectrum of [4-(9-anthryl)phenyl]diphenylphosphine oxide **1** in $CDCl_3$.

$^{13}C$ NMR (500 MHz, $CDCl_3$, 25 °C): $\delta$ 142.9 (d, $J$ = 11.5 Hz, Phenyl($C^5$)), 135.4 (s, Phenyl($C^6H$)), 132.9 (s, Phenyl($C^8$)), 132.3-132.1 (m, Phenyl($PC^1$), Phenyl($C^7H$)), 131.6 (s, Anth($C^9$)), 131.5 (s, Anth($C^{16}H$)), 131.3 (s, Anth($C^{10}$)), 129.9 (s, Anth($C^{15}$)), 128.7 (s, Phenyl($C^2H$)), 128.6 (s, Phenyl($C^3H$)), 128.4 (s, Phenyl($C^4H$)), 127.2 (s, Anth($C^{11}H$)), 126.3 (s, Anth($C^{12}H$)), 125.7 (s, Anth($C^{13}H$)), 125.2 (s, Anth($C^{14}H$)) ppm.

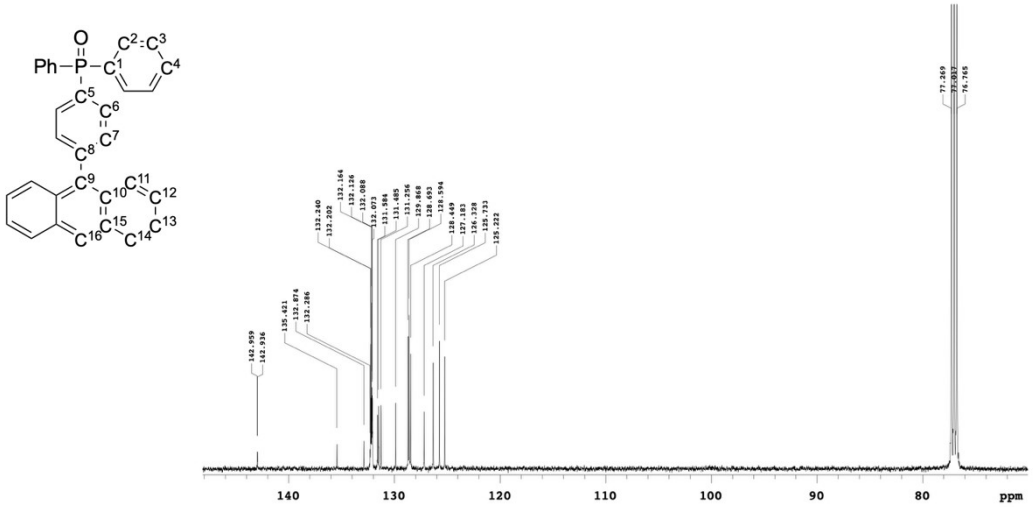


Fig. S3. $^{13}C$ NMR spectrum of **1** in $CDCl_3$.

$^{31}P$ NMR(202 MHz,$CDCl_3$, 25 °C): $\delta$ 29.3 ppm.

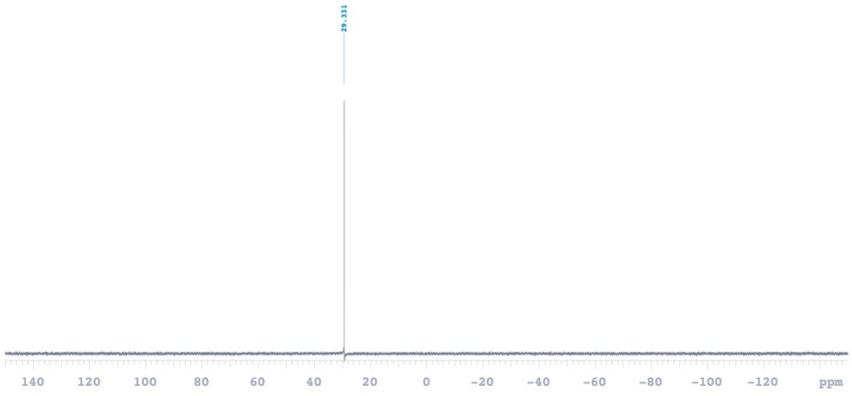


Fig. S4. $^{31}P$ NMR spectrum of **1** in $CDCl_3$.

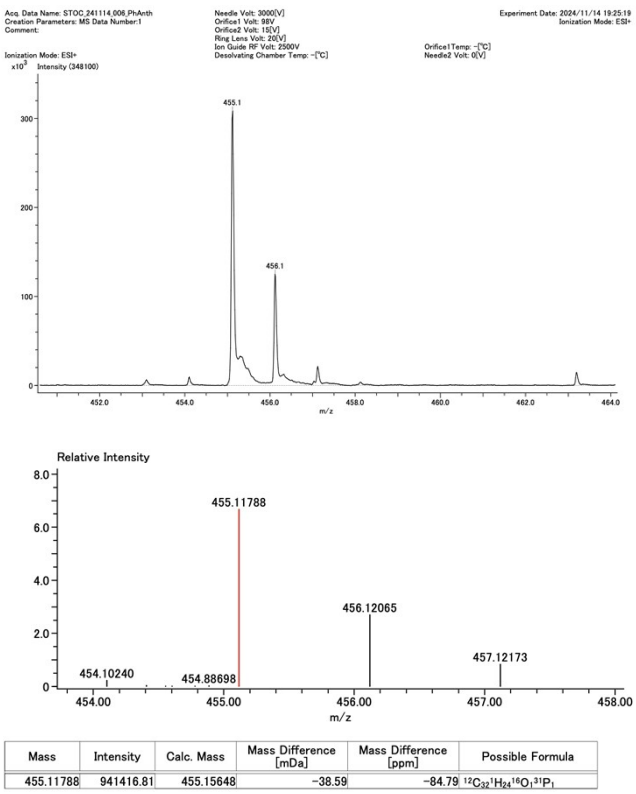


| Mass | Intensity | Calc. Mass | Mass Difference [mDa] | Mass Difference [ppm] | Possible Formula |
|---|---|---|---|---|---|
| 455.11788 | 941416.81 | 455.15648 | -38.59 | -84.79 | $^{12}C_{32}{}^{1}H_{24}{}^{16}O_1{}^{31}P_1$ |

Fig. S5. ESI-MS spectrum of **1** in $CHCl_3$/MeOH. MS (ESI-TOF): *m/z* Calcd for $C_{32}H_{24}OP$: 455.15648. Found: 455.11788.

***Synthesis of (4-bromophenyl)diphenylphosphine oxide***

Under a $N_2$ atmosphere, 1,4-dibromobenzene (1.97 g, 8.36 mmol) were dissolved in anhydrated tetrahydrofuran (20 mL). The solution was cooled to –78℃ and added *sec*-BuLi (1.2 M in *n*-hexane, 10 mL, 12 mmol). After stirred for 30 min, chlorodiphenylphosphine (1.5 mL, 8.2 mmol) was added to mixture and reacted at room temperature for 2 hours. Subsequently, water was incorporated to deactivate any residual *sec*-BuLi, and then hydrogen peroxide (30%, 1.5 mL) was added and stirred for 30 minutes. After the reaction, the mixture was quenched with water, extracted with chloroform, and washed with brine. The organic layer was dried over anhydrous $Na_2SO_4$ and evaporated under reduced pressure. Then, the crude product was purified by column chromatography over silica gel using hexane/EtOAc (2:1, 1:1 *v*/*v*) as eluent. Target molecule was obtained as white solid (2.04 g, 69.7%).

$^1$H NMR (500 MHz, $CDCl_3$, 25 ℃): $\delta$ 7.67-7.63 (m, 4H), 7.62-7.60 (dd, $J$ = 2.5 Hz, 2H), 7.58-7.51 (m, 4H), 7.49-7.46(t, 4H) ppm.

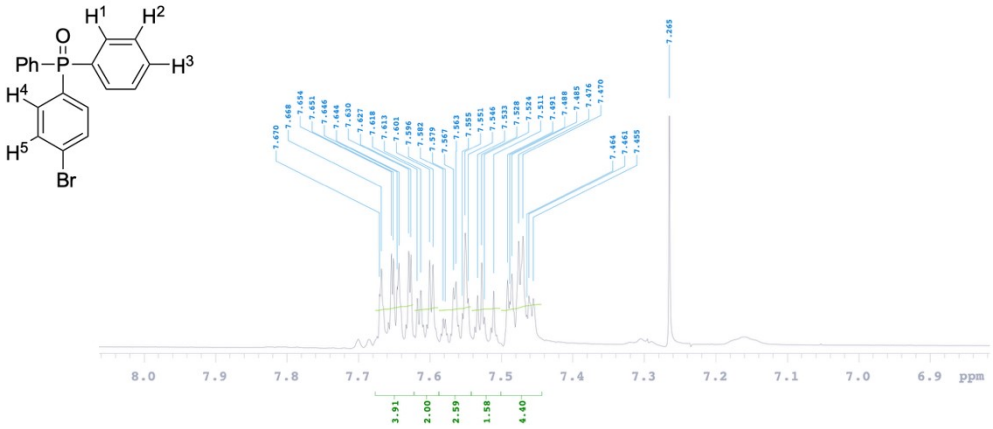


Fig. S6. $^1$H NMR spectrum of (4-Bromophenyl)diphenylphosphine oxide in $CDCl_3$.

$^{31}$P NMR(202 MHz,$CDCl_3$, 25 ℃): $\delta$ 28.7 ppm.

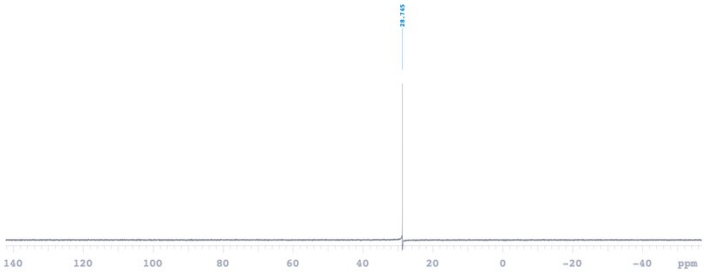


Fig. S7. $^{31}$P NMR spectrum of (4-Bromophenyl)diphenylphosphine oxide in $CDCl_3$.

***Synthesis of [4-(1-pyrenyl)phenyl]diphenylphosphine oxide 3***

A mixture of (4-bromophenyl)diphenylphosphine oxide (0.360 g, 1.01 mmol), 1-Pyreneboronic acid (0.502 g, 2.04 mmol), $Pd(PPh_3)_4$ (0.123 g, 0.106 mmol), $K_2CO_3$ aq. (0.687 g, 4.97 mmol) in toluene/MeOH (*v*/*v*= 8 mL/2 mL) was refluxed under $N_2$ at 110°C for overnight. After cooling to room temperature, the mixture was filtrated through Celite, quenched with water, extracted with chloroform, and washed with brine. The organic layer was dried over anhydrous $Na_2SO_4$ and evaporated under reduced pressure. Then, the crude product was purified by column chromatography over silica gel using $CHCl_3$/EtOAc (20:1 *v*/*v*) as eluent. Compound **3** was obtained Light brown solid (0.303 g, 62.9%).

$^1$H NMR (500 MHz, $CDCl_3$, 25 °C): $\delta$ 8.26-8.20 (m, 3H($H^9$, $H^{10}$, $H^{11}$)), 8.15-8.11 (m, 3H($H^8$, $H^{12}$, $H^{13}$)), 8.10-8.03 (m, 2H($H^6$, $H^7$), 7.98 (d, *J* = 8.0 Hz, 1H($H^{14}$)), 7.90-7.80 (m, 6H($H^1$, $H^4$)), 7.76 (dd, *J* = 2.5 Hz, 2H($H^5$)), 7.62 (td, *J* = 1.5, 0.2, 1.5 Hz, 2H($H^3$)), 7.55 (td, *J* = 3, 4 Hz, 4H($H^2$)) ppm.

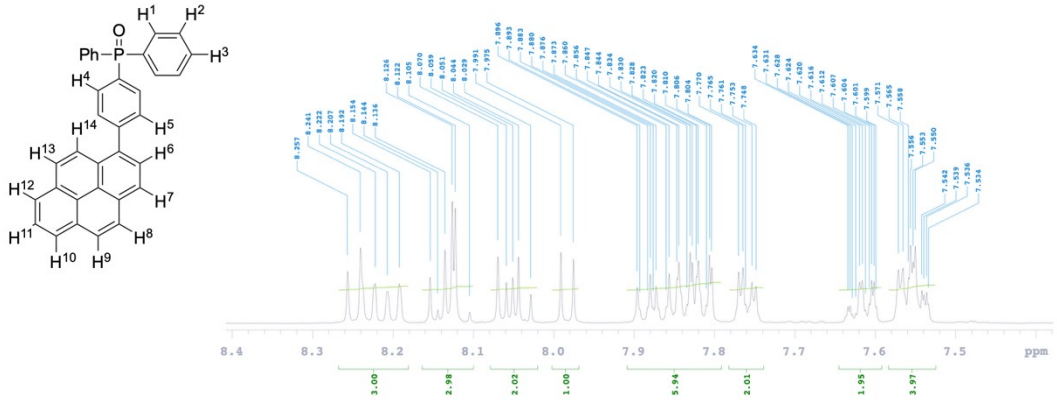


Fig. S8. $^1$H NMR spectrum of [4-(1-pyrenyl)phenyl]diphenylphosphine oxide **3** in $CDCl_3$.

$^{13}$C NMR (500 MHz, $CDCl_3$, 25 °C): $\delta$ 145.0 (s, Phenyl($C^5$)), 136.2 (s, Phenyl($C^6$H)), 133.0 (s, Phenyl($C^8$)), 132.2 (d, *J* = 42 Hz, Phenyl($C^7$H)), 132.1 (s, Phenyl($C^1$)), 131.4 (s, Pyre($C^9$)), 131.0 (s, Pyre($C^{11}$)), 130.9 (s, Pyre($C^{12}$)), 130.8 (s, Pyre($C^{14}$)), 130.7 (s, Pyre($C^{10}$)), 128.7 (s, Phenyl($C^2$H)), 128.6 (s, Phenyl($C^3$H)), 128.4 (s, Phenyl($C^4$H)), 127.9 (s, Pyre($C^{17}$)), 127.8 (s, Pyre($C^{15}$)), 127.4 (s, Pyre($C^{18}$)), 126.2 (s, Pyre($C^{16}$)),

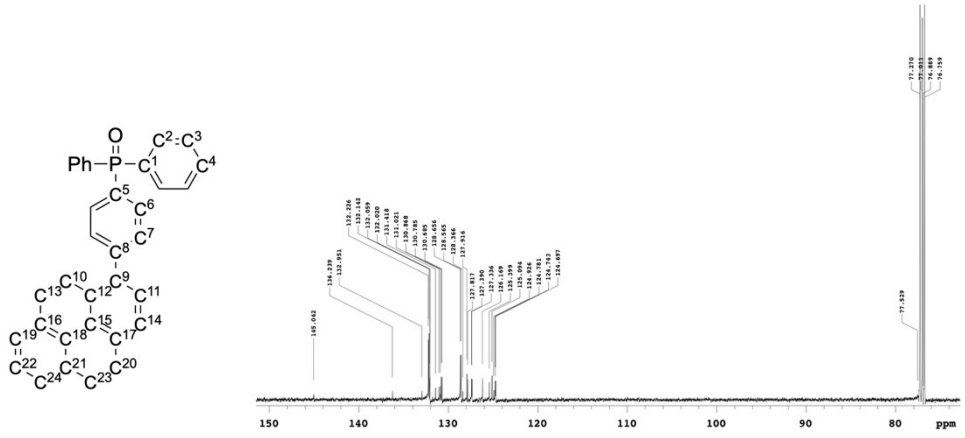

125.4 (s, Pyre($C^{20}$)), 125.1 (s, Pyre($C^{19}$)), 124.9 (s, Pyre($C^{21}$)), 124.8 (s, Pyre($C^{22}$)), 124.7(s, Pyre($C^{23}$)), 124.7 (s, Pyre($C^{24}$)) ppm.

Fig. S9. $^{13}C$ NMR spectrum of **3** in $CDCl_3$.

$^{31}P$ NMR(202 MHz,$CDCl_3$, 25 ℃): $\delta$ 29.2 ppm.

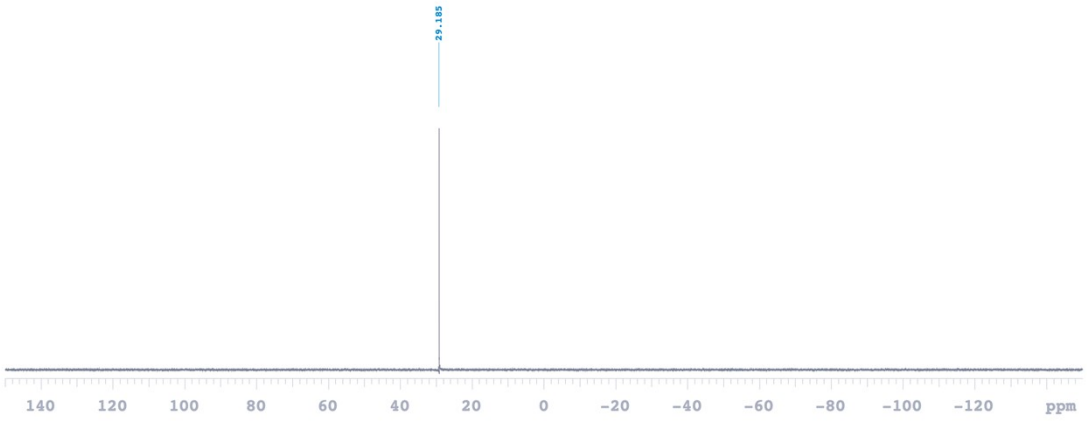


Fig. S10. $^{31}P$ NMR spectrum of **3** in $CDCl_3$.

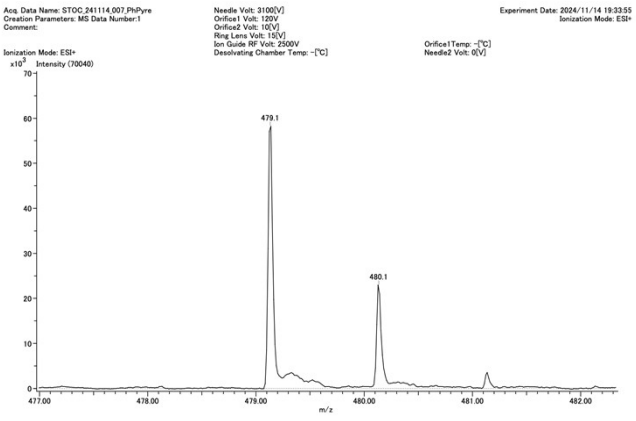

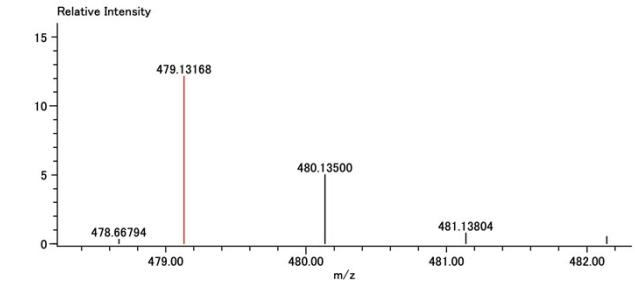


| Mass | Intensity | Calc. Mass | Mass Difference [mDa] | Mass Difference [ppm] | Possible Formula |
|---|---|---|---|---|---|
| 479.13168 | 121527.14 | 479.15648 | −24.79 | −51.74 | $^{12}C_{34}{}^{1}H_{24}{}^{16}O_{1}{}^{31}P_{1}$ |

Fig. S11. ESI-MS spectrum of **3** in $CHCl_3$/MeOH. MS (ESI-TOF): MS (ESI-TOF): *m/z* Calcd for $C_{34}H_{24}OP$: 479.15648. Found: 479.13168.

***Synthesis of 9-(2,2-dibromoehynyl)anthracene***

Triphenylphosphine (3.74 g, 14.2 mmol) dissolved in dichloromethane (10 mL) was added dropwise to 9-anthracenecarbaldehyde (0.461 g, 2.24 mmol) and carbon tetrabromide (3.29 g, 9.91 mmol) in dichloromethane (20 mL) at 0°C. The mixture was stirred at this temperature for 30 minutes. The mixture was returned to room temperature and stirred for 2 hours. After the reaction, the mixture was quenched with water, extracted with chloroform, and washed with brine. The organic layer was dried over anhydrous $Na_2SO_4$ and evaporated under reduced pressure. Then, the crude product was purified by column chromatography over silica gel using hexane as eluent. Target molecule was obtained as yellow solid (0.815 g, 99.9%).

$^1$H NMR (500 MHz, $CDCl_3$, 25 °C): $\delta$ 8.51 (s, 1H($H^6$)), 8.12 (s, 1H($H^1$)), 8.08-8.03 (m, 4H($H^2$, $H^5$)), 7.56 (td, $J$ = 1, 1.5, 7 Hz, 2H($H^4$)), 7.50 (td, $J$ = 1, 1.5, 8 Hz, 2H($H^3$)) ppm.

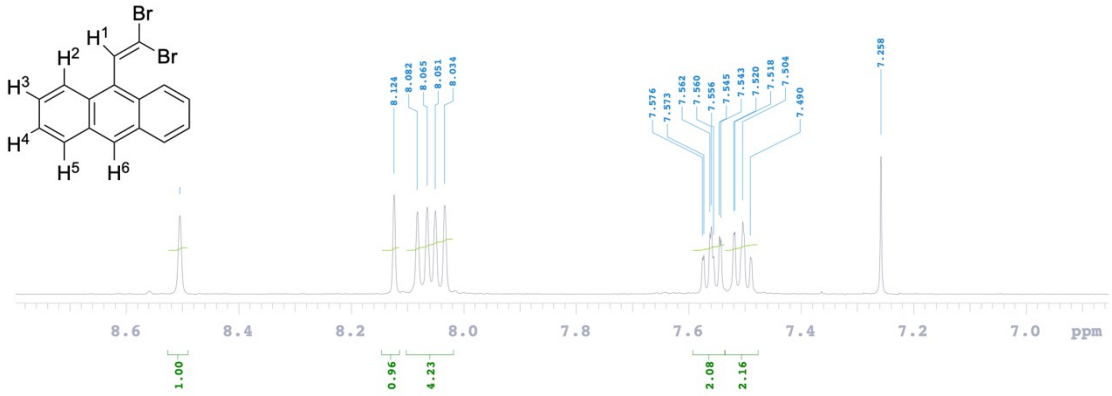


Fig. S12. $^1$H NMR spectrum of 9-(2,2-dibromoehynyl)anthracene in $CDCl_3$.

***Synthesis of 9-ethynylanthracene***

A mixture of 9-(2,2-dibromoehynyl)anthracene (0.360 g, 0.995 mmol), succinimide (0.301 g, 3.04 mmol), $K_2CO_3$ (0.837 g, 6.05 mmol) in DMSO (10 mL) was refluxed at 90 ℃ for overnight. After cooling to room temperature, the mixture was quenched with water, extracted with ethyl acetate, and washed with brine. The organic layer was dried over anhydrous $Na_2SO_4$ and evaporated under reduced pressure. Then, the crude product was purified by column chromatography over silica gel using hexane as eluent. Target molecule was obtained as yellow oil (0.151 g, 74.9%).

$^1$H NMR (500 MHz, $CDCl_3$, 25 ℃): $\delta$ 8.58 (dd, $J$ = 0.5, 8.5 Hz, 2H($H^2$)), 8.45 (s, 1H($H^6$)), 8.01 (d, $J$ = 8.5 Hz, 2H($H^5$)), 7.59 (td, $J$ = 1.0, 1.5, 6.5 Hz, 2H($H^4$)), 7.50 (td, $J$ = 1.0, 2.0, 6.5 Hz, 2H($H^3$)), 3.98 (s, 1H($H^1$)) ppm.

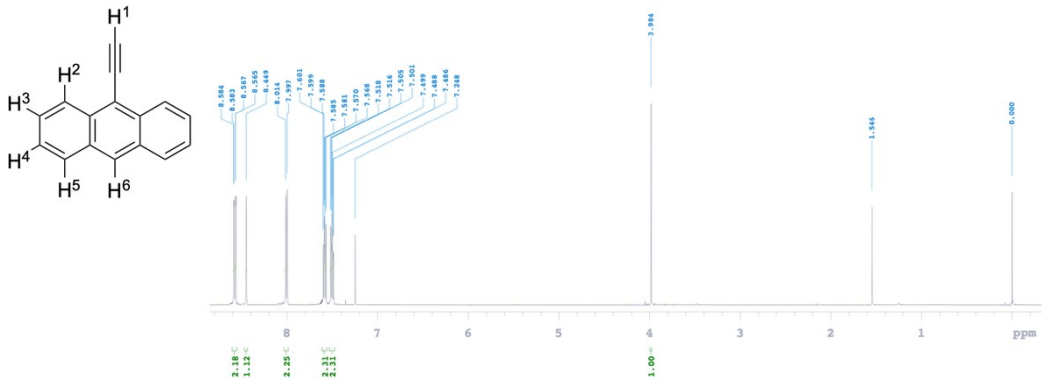


Fig. S13. $^1$H NMR spectrum of 9-ethynylanthracene in $CDCl_3$.

***Synthesis of [2-(9-anthryl)ethynyl]diphenylphosphineoxide 2***

Under a $N_2$ atmosphere, 9-ethynylanthracene (0.145 g, 0.731 mmol) were dissolved in anhydrated tetrahydrofuran (10 mL). The solution was cooled to –78℃ and added *sec*-BuLi (1.2 M in *n*-hexane, 1 mL, 1.2 mmol). After stirred for 30 min, chlorodiphenylphosphine (0.14 mL, 0.76 mmol) was added to mixture and reacted at room temperature for 2 hours. Subsequently, water was incorporated to deactivate any residual *sec*-BuLi, and then hydrogen peroxide (30%, 1.5 mL) was added and stirred for 40 minutes. After the reaction, the mixture was quenched with water, extracted with chloroform, and washed with brine. The organic layer was dried over anhydrous $Na_2SO_4$ and evaporated under reduced pressure. Then, the crude product was purified by column chromatography over silica gel using hexane/EtOAc (1:1 *v*/*v*) as eluent. Compound **2** was obtained as yellow solid (0.215 g, 73.1%).

$^1$H NMR (500 MHz, $CDCl_3$, 25 ℃): $\delta$ 8.55 (s, 1H($H^8$)), 8.44 (dd, $J$ = 1.0, 8.5 Hz, 2H($H^4$)), 8.09-8.03 (m, 6H($H^1$, $H^7$)), 7.61-7.53 (m, 10H($H^2$, $H^3$, $H^5$, $H^6$)) ppm.

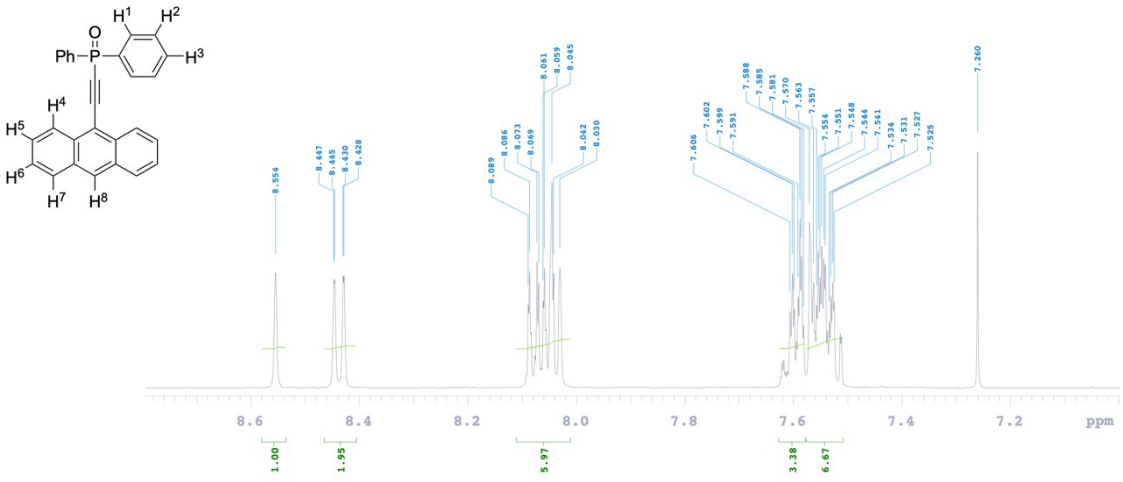


Fig. S14. $^1$H NMR spectrum of [2-(9-anthryl)ethynyl]diphenylphosphineoxide **2** in $CDCl_3$.

$^{13}$C NMR (500 MHz, $CDCl_3$, 25 ℃): $\delta$ 133.9 (s, Anth($C^{14}$)), 133.8 (s, Anth($C^{13}$)), 132.8 (s, Anth($C^{12}$)), 132.4 (d, $J$ = 11.5 Hz, Phenyl($C^1$H)), 131.1 (d, $J$ = 45.5 Hz, Phenyl($C^2$H)), 130.8(s, Phenyl($C^3$H)), 129.0 (s, Anth($C^9$H)), 128.8 (d, $J$ = 53.5 Hz, Phenyl($C^4$H)), 128.0 (s, Anth($C^{10}$H)), 126.0 (d, $J$ = 8 Hz, Anth($C^{11}$H)), 113.1 (s, Anth($C^8$H)), 103.2 (d, $J$ = 118 Hz, Anth($C^7$)), 94.4 (s, C≡C($C^5$)), 93.1 (s, C≡C($C^6$))ppm.

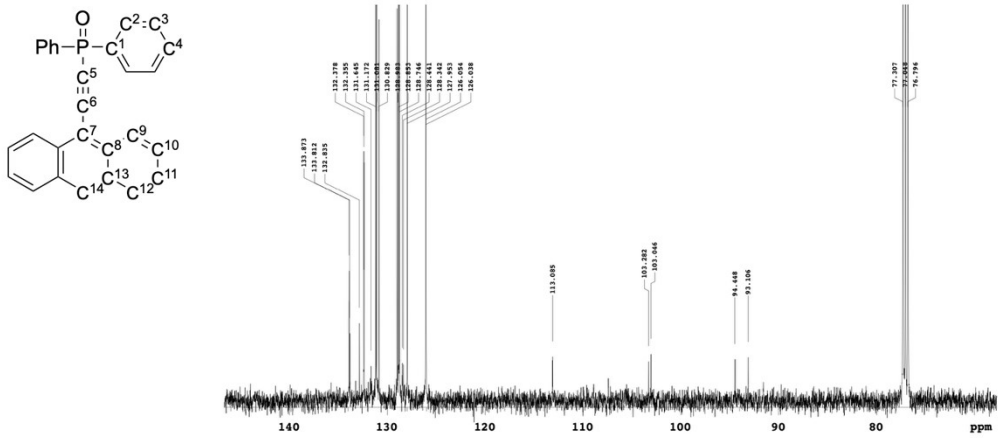


Fig. S15. $^{13}C$ NMR spectrum of **2** in $CDCl_3$.

$^{31}P$ NMR (202 MHz,$CDCl_3$, 25 ℃): $\delta$ 8.40 ppm.

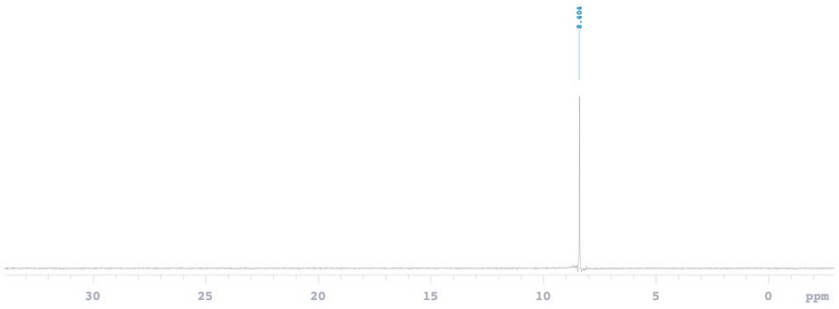


Fig. S16. $^{31}P$ NMR spectrum of **2** in $CDCl_3$.

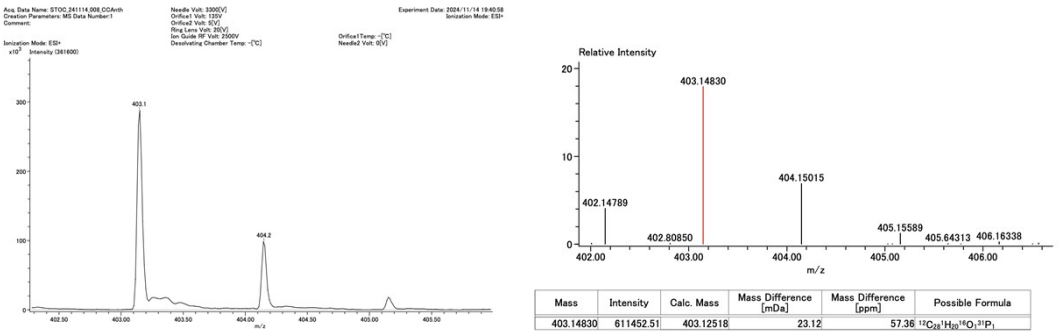


Fig. S17. ESI-MS spectrum of **2** in $CHCl_3$/MeOH. MS (ESI-TOF): MS (ESI-TOF): MS (ESI-TOF): *m/z* Calcd for $C_{28}H_{20}OP$: 403.12518. Found: 403.14830.

***Synthesis of 1-(2,2-dibromoethenyl)pyrene***

Triphenylphosphine (5.07 g, 21.0 mmol) dissolved in dichloromethane (40 mL) was added dropwise to 1-pyrenecarbaldehyde (0.695 g, 3.02 mmol) and Carbon tetrabromide (5.07 g, 15.3 mmol) in dichloromethane (30 mL) at 0°C. The mixture was stirred at this temperature for 30 minutes. The mixture was returned to room temperature and stirred for 2 hours. After the reaction, the mixture was quenched with water, extracted with chloroform, and washed with brine. The organic layer was dried over anhydrous $Na_2SO_4$ and evaporated under reduced pressure. Then, the crude product was purified by column chromatography over silica gel using hexane/EtOAc (20:1, 10:1 *v*/*v*) as eluent. Target molecule was obtained as light yellow solid (2.19 g, 99.9%).

$^1$H NMR (500 MHz, $CDCl_3$, 25 °C): $\delta$ 8.24-8.11 (m, 8H), 8.08-8.02 (m, 2H) ppm.

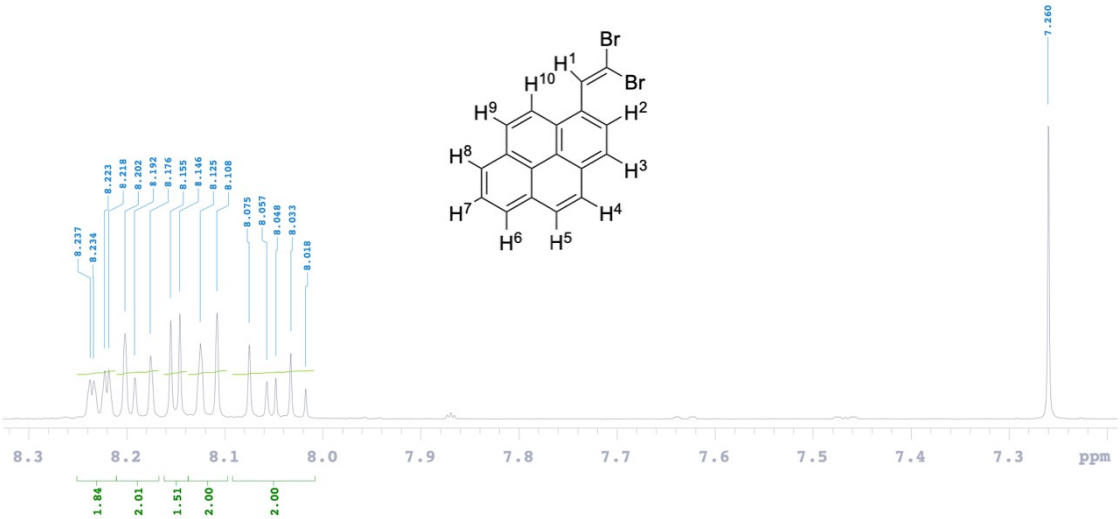


Fig. S18. $^1$H NMR spectrum of 1-(2,2-dibromoethenyl)pyrene in $CDCl_3$.

***Synthesis of 1-ethynylpyrene***

A mixture of 1-(2,2-dibromoehynyl)pyrene (2.07 g, 5.37 mmol), succinimide (1.66 g, 16.7 mmol), $K_2CO_3$ (4.47 g, 32.4 mmol) in DMSO (46 mL) was refluxed at 90 ℃ for overnight. After cooling to room temperature, the mixture was quenched with water, extracted with ethyl acetate, and washed with brine. The organic layer was dried over anhydrous $Na_2SO_4$ and evaporated under reduced pressure. Then, the crude product was purified by column chromatography over silica gel using hexane/EtOAc (10:1 *v*/*v*) as eluent. Target molecule was obtained as yellow solid (1.85 g, 99.9%).

$^1$H NMR (500 MHz, $CDCl_3$, 25 ℃): $\delta$ 8.60 (d, $J$ = 9.5 Hz, 1H($H^{10}$)), 8.23-8.16 (m, 4H($H^5$, $H^6$, $H^7$, $H^8$)), 8.10 (d, $J$ = 8.5 Hz, 2H($H^2$, $H^3$)), 8.05-8.01 (m, 2H($H^4$, $H^9$)), 3.63 (s,1H($H^1$)) ppm.

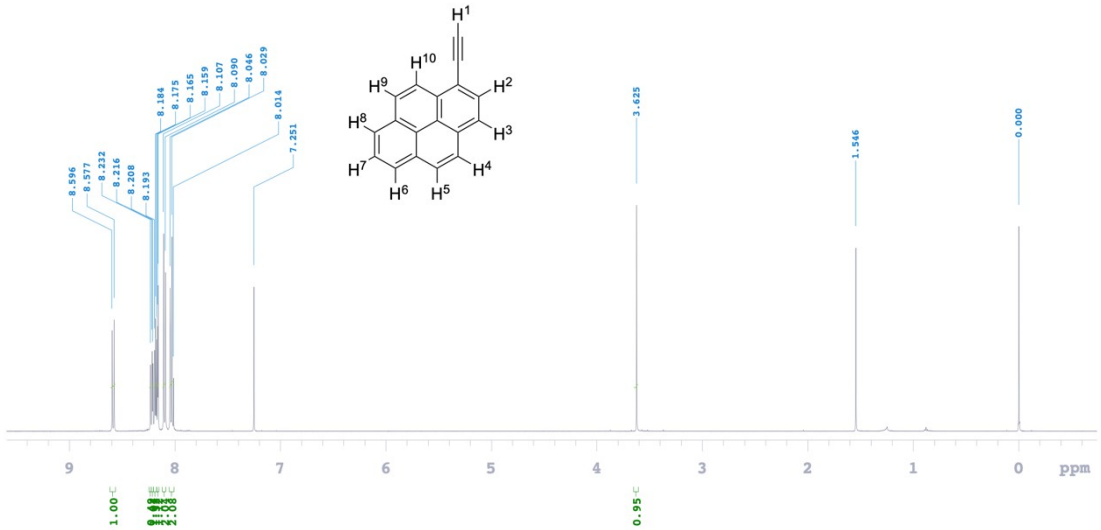


Fig. S19. $^1$H NMR spectrum of 1-ethynylpyrene in $CDCl_3$.

***Synthesis of [2-(1-pyrenyl)ethynyl]diphenylphosphineoxide 4***

Under a $N_2$ atmosphere, 1-ethynylpyrene (0.141 g, 0.623 mmol) were dissolved in anhydrated tetrahydrofuran (10 mL). The solution was cooled to –78 ℃ and added *sec*-BuLi (1.2 M in *n*-hexane, 0.7 mL, 0.8 mmol). After stirred for 30 min, chlorodiphenylphosphine (0.14 mL, 0.76 mmol) was added to mixture and reacted at room temperature for 2 hours. Subsequently, water was incorporated to deactivate any residual *sec*-BuLi, and then hydrogen peroxide (30%, 1.5 mL) was added and stirred for 30 minutes. After the reaction, the mixture was quenched with water, extracted with chloroform, and washed with brine. The organic layer was dried over anhydrous $Na_2SO_4$ and evaporated under reduced pressure. Then, the crude product was purified by column chromatography over silica gel using hexane/EtOAc (20:1, 10:1, 1:1 *v*/*v*) as eluent. Compound **4** was obtained as yellow solid (0.244, 91.9%).

$^1$H NMR (500 MHz, $CDCl_3$, 25 ℃): $\delta$ 8.48 (d, $J$ = 9.5 Hz, 1H($H^{12}$)), 8.26-8.24 (m, 3H($H^9$, $H^6$, $H^{10}$)), 8.20-8.16 (m, 2H($H^8$, $H^7$)), 8.13 (d, $J$ = 8.0 Hz, 1H($H^4$)), 8.10-8.03 (m, 6H($H^1$, $H^5$, $H^{11}$, ), 7.62-7.59 (m,2H($H^3$)), 7.58-7.54 (m, 4H($H^2$)) ppm.

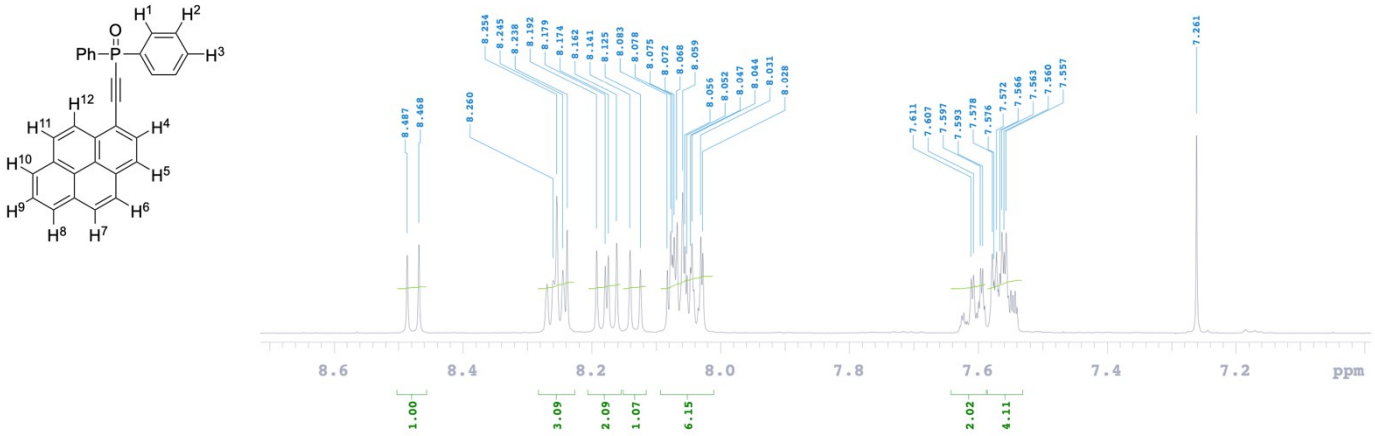


Fig. S20. $^1$H NMR spectrum of **4** in $CDCl_3$.

$^{13}$C NMR (500 MHz, $CDCl_3$, 25 ℃): $\delta$ 133.8 (s, Pyre($C^{22}$H)), 133.2 (s, Pyre($C^{21}$H)), 132.9 (s, Pyre($C^{20}$H)), 132.8 (s, Pyre($C^8$H)), 132.3 (d, $J$ = 11.5 Hz, Phenyl($C^1$)), 131.1 (d, $J$ = 41.5 Hz, Phenyl($C^2$H)), 131.0 (s, Phenyl($C^3$H)), 130.7 (s, Pyre($C^{11}$H)), 130.4 (d, $J$ = 7.5 Hz, Pyre($C^{19}$)), 128.8 (d, $J$ = 15 Hz, Pyre($C^{17}$H)), 128.7 (d, $J$ = 57 Hz, Phenyl($C^4$H)), 127.1 (s, Pyre($C^{18}$H)), 126.6 (s, Pyre($C^{14}$)), 126.4 (d, $J$ = 38 Hz, Pyre($C^{16}$)), 124.7 (s, Pyre($C^{15}$)), 124.4 (s, Pyre($C^{13}$)), 124.1 (s, Pyre($C^{12}$H)), 123.9 (s, Pyre($C^9$H)), 113.6 (d, $J$ = 15.5 Hz, Pyre($C^{10}$)), 105.2 (d, $J$ = 122.5 Hz, Pyre($C^7$)), 88.8 (s, C≡C($C^5$)), 87.5 (s, C≡C($C^6$)) ppm.

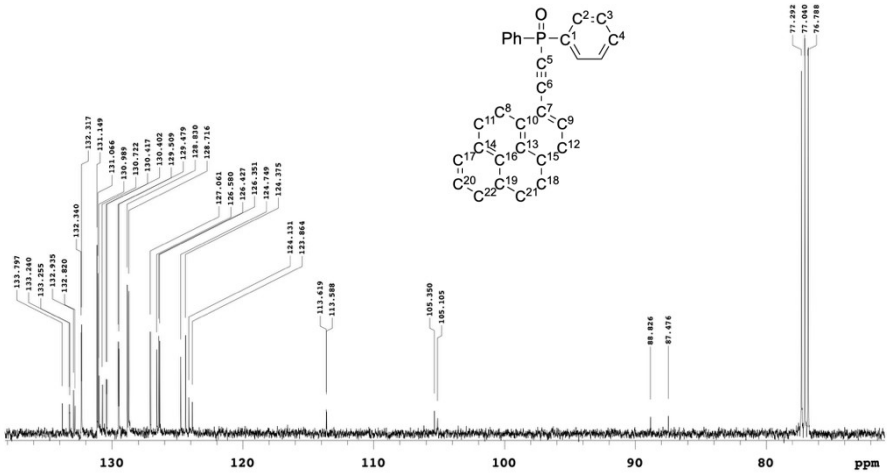


Fig. S21. $^{13}C$ NMR spectrum of **4** in $CDCl_3$.

$^{31}P$ NMR (202 MHz,$CDCl_3$, 25 ℃): $\delta$ 8.46 ppm.

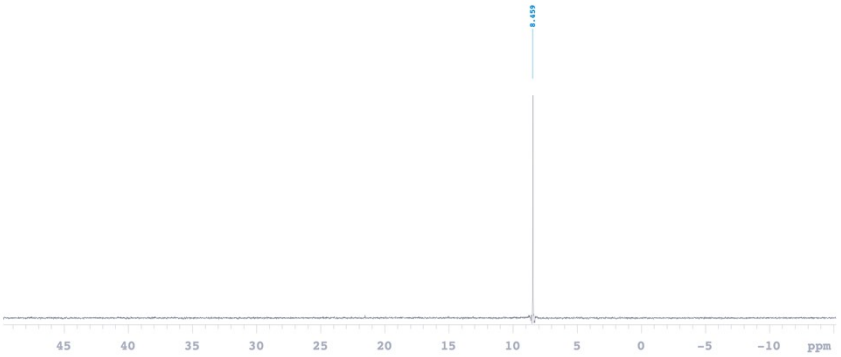


Fig. S22. $^{31}P$ NMR spectrum of **4** in $CDCl_3$.

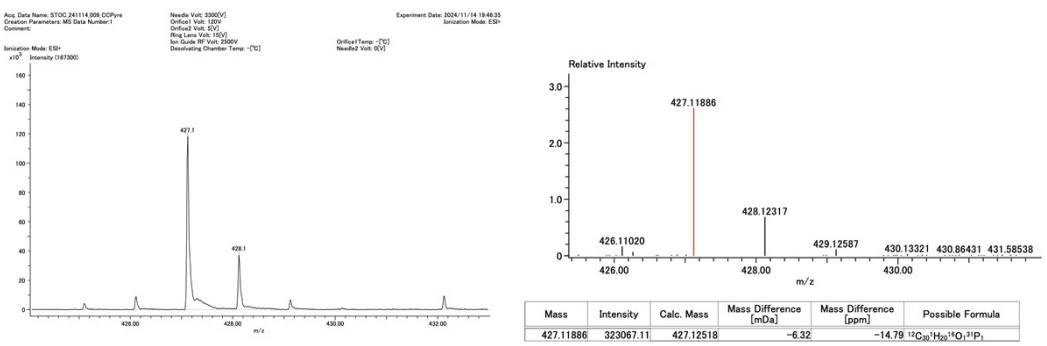


Fig. S23. ESI-MS spectrum of **4** in $CHCl_3$/MeOH. MS (ESI-TOF): MS (ESI-TOF): MS (ESI-TOF): *m/z* Calcd for $C_{30}H_{20}OP$: 427.12518. Found: 427.11886.

**Single Crystal X-ray Diffraction.** Single crystal X-ray diffraction (SCXRD) data for crystals **1**, **2a**, **2b**, **3a**, **3c**, **4** were collected on a RIGAKU Oxford Diffraction XtaLAB Pro equipped with a Dectris PILATUS 200 K HPAD detector and microfocus sealed tube CuKα radiation with mirror optics ($\lambda$ = 1.54184 Å). The diffraction data were integrated using CrysAlisPro[1] and corrected for absorption effects using a combination of empirical (ABSPACK) and numerical corrections. The structures were solved using SHELXT and refined by full-matrix least-squares analysis (SHELXL) using the OLEX2 program package.[2] Unless otherwise indicated, all non-hydrogen atoms were refined anisotropically. All the hydrogen atom positions were constrained to ideal geometries and refined using fixed isotropic displacement parameters (in terms of the riding model). X-ray diffraction images for crystals **1** and **2b** were collected using an EIGER 4M detector with synchrotron radiation at a wavelength of 0.80000 Å at the BL26B1 station of SPring-8 (Hyogo, Japan). The distance between the crystal and detector was 50 mm. Images were processed using HKL2000 (HKL Research) or the XDS program package. The structural solution and refinement were performed using SHELXS-97 and SHELXL-2014/7 (Sheldrick).[3]

Table S1. Crystallization conditions.

| | Recrystallization solvent | Temperature (°C) | Crystal shape | SCXRD | PXRD |
|---|---|---|---|---|---|
| **1** | $CHCl_3$, MeOH | 5[a], 25, 40 [b] |  | ○ | ○ |
| **2a** | EtOH, MeOH, Acetone, MeCN, Toluene, DMF | 5, 25, 40 |  | ○ | ○ |
| **2b** | AcOEt | 5, 25 |  | ○ | ○ |
| **3** | EtOH, MeOH, Acetone, MeCN, Toluene, DMF | 5, 25, 40 |  | ○ | ○ |
| **4a** | EtOH, MeOH, Acetone, MeCN, Toluene | 5, 25, 40 |  | ○ | ○ |
| **4b** | DMF | 5 [a] |  | ○ | △[c] |

a. The solution was placed in a sample tube and stored in the refrigerator.
b. The solution was placed in a sample tube and stored in a hot water bath.
c. During sample preparation for PXRD, grinding operations cause slight polymorphic transitions, resulting in reduced purity.

Table S2. Crystal date of [4-(9-Anthryl)phenyl]diphenylphosphine oxide **1**

| | |
|---|---|
| formula | $C_{32}H_{23}OP$ |
| formula weight | 454.47 |
| crystal system | monoclinic |
| space group | $P2_1/c$ |
| $a$ (Å), $\alpha$ (°) | 9.66347(14), 90 |
| $b$ (Å), $\beta$ (°) | 27.2681(3), 115.74(2) |
| $c$ (Å), $\gamma$ (°) | 9.86176(18), 90 |
| $V$ (Å$^3$) | 2347.92(7) |
| $Z$ | 4 |
| $R$ | 0.0361, 0.0933 |
| $D_{calc}$ (gm$^{-3}$) | 1.286 |
| $\mu$ (mm$^{-1}$) | 1.205 |
| GOF | 1.045 |
| $R_1$, $wR_2$ (all data) | 0.0398, 0.0957 |
| CCDC number | 2432548 |

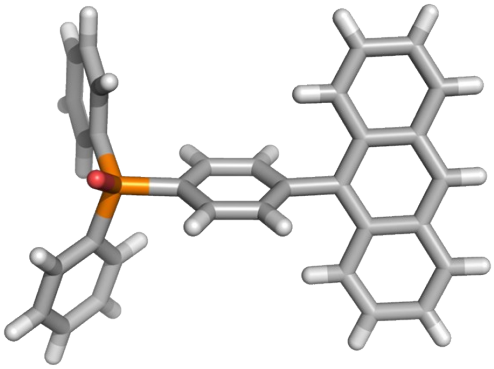

Fig. S24. Crystal structure of [4-(9-Anthryl)phenyl]diphenylphosphine oxide **1** in the stick model. Crystal model was created by the PyMOL molecular graphics system. (Gray: C, White: H, Orange: P, Red: O)

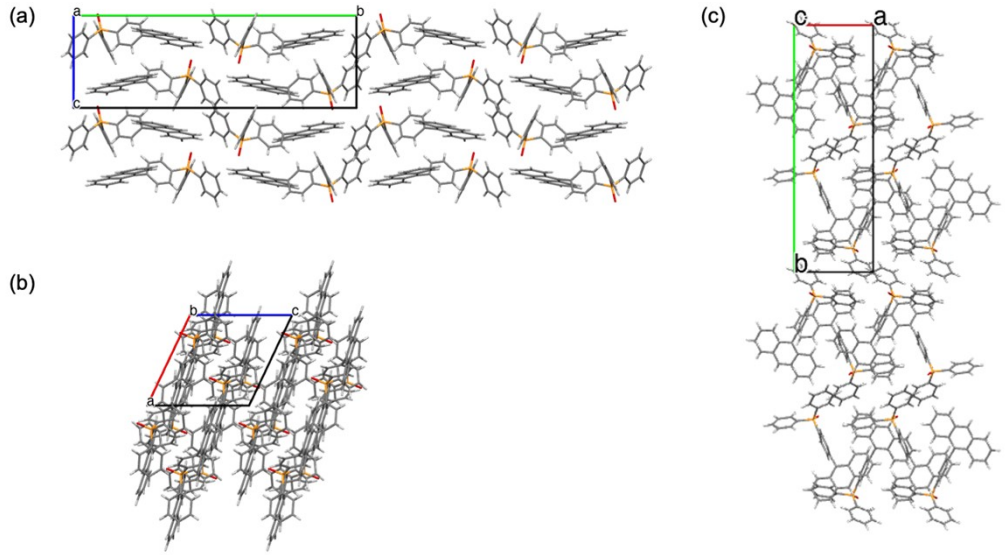


Fig. S25. Crystal packing of **1** viewed from each direction of *a*, *b*, and *c* axes.

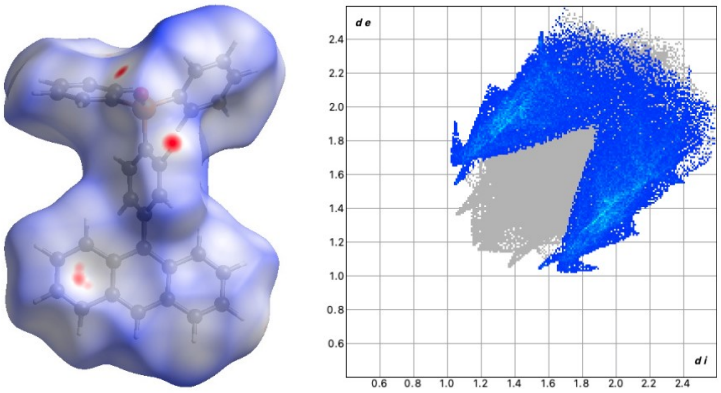


Fig. S26. Selective highlighting of C···H contacts on the Hirshfeld surface of axle of **1** mapped with $d_{norm}$ surface (left), and fingerprint plots of axle of **1** resolved into all contacts (right). The full fingerprint appears beneath decomposed plots as a gray shadow.

Table S3. Crystal date of [4-(1-pyrenyl)phenyl]diphenylphosphine oxide **3**

| | |
|---|---|
| formula | $C_{34}H_{23}OP$ |
| formula weight | 478.49 |
| crystal system | monoclinic |
| space group | $P2_1/c$ |
| $a$ (Å), $\alpha$ (°) | 17.2834(4), 90 |
| $b$ (Å), $\beta$ (°) | 9.4529(2), 99.788(2) |
| $c$ (Å), $\gamma$ (°) | 14.7171(3), 90 |
| $V$ (Å$^3$) | 2369.48(10) |
| $Z$ | 4 |
| $R$ | 0.0382, 0.1282 |
| $D_{calc}$ (gm$^{-3}$) | 1.341 |
| $\mu$ (mm$^{-1}$) | 1.225 |
| GOF | 1.049 |
| $R_1$, $wR_2$ (all data) | 0.0460, 0.1352 |
| CCDC number | 2432551 |

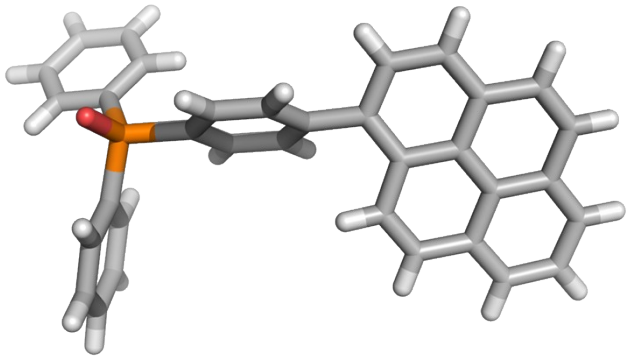

Fig. S27. Crystal structure of [4-(1-pyrenyl)phenyl]diphenylphosphine oxide **3** in the ball and stick model. Crystal model was created by the PyMOL molecular graphics system. (Gray: C, White: H, Orange: P, Red: O)

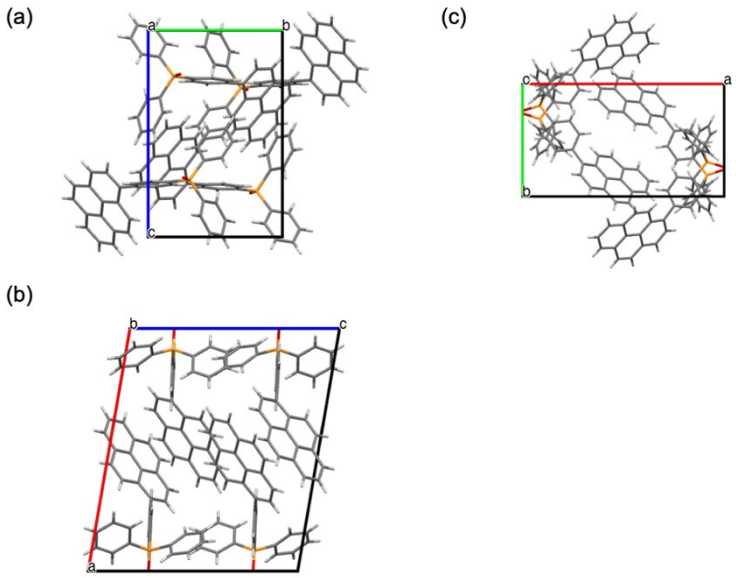


Fig. S28. Crystal packing of **3** viewed from each direction of *a*, *b*, and *c* axes.

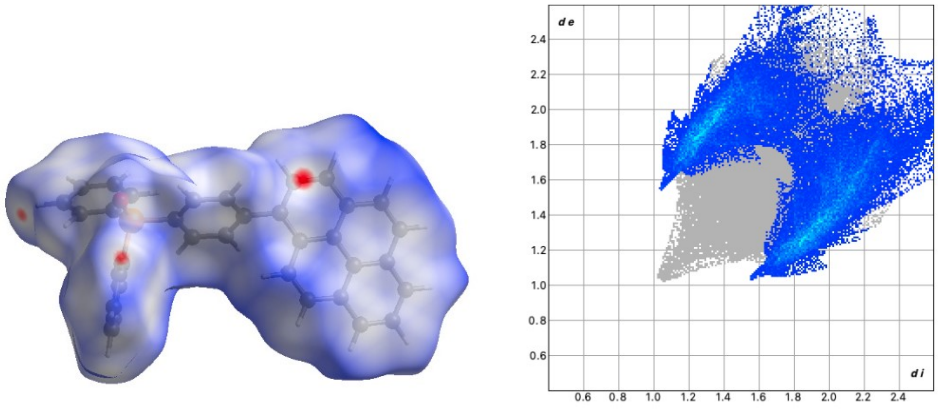


Fig. S29. Selective highlighting of C···H contacts on the Hirshfeld surface of axle of **3** mapped with $d_{norm}$ surface (left), and fingerprint plots of axle of **3** resolved into C–H contacts (right). Contribution ratio of the C–H interactions was calculated to be 40.9%. The full fingerprint appears beneath decomposed plots as a gray shadow.

Table S4. Crystal date of [2-(9-anthryl)ethynyl]diphenylphosphine oxide **2a** and **2b**.

| | **2a** | **2b** |
|---|---|---|
| formula | $C_{28}H_{19}OP$ | $C_{28}H_{19}OP$ |
| formula weight | 402.40 | 402.40 |
| crystal system | monoclinic | triclinic |
| space group | $P2_1/c$ | $P$-1 |
| $a$ (Å), $\alpha$ (°) | 9.88921(8), 90 | 9.8161(8), 109.508(5) |
| $b$ (Å), $\beta$ (°) | 23.1560(2), 92.3493(7) | 10.1226(5), 99.186(7) |
| $c$ (Å), $\gamma$ (°) | 8.93733(7), 90 | 11.6958(9), 93.455(6) |
| $V$ (Å$^3$) | 2044.87(3) | 1073.31(13) |
| $Z$ | 4 | 2 |
| $R$ | 0.0419, 0.1155 | 0.0809, 0.2471 |
| $D_{calc}$ (gm$^{-3}$) | 1.307 | 1.245 |
| $\mu$ (mm$^{-1}$) | 1.313 | 1.251 |
| GOF | 1.040 | 1.184 |
| $R_1$, $wR_2$ (all data) | 0.0434, 0.1171 | 0.1137, 0.3249 |
| CCDC number | 2432549 | 2432550 |

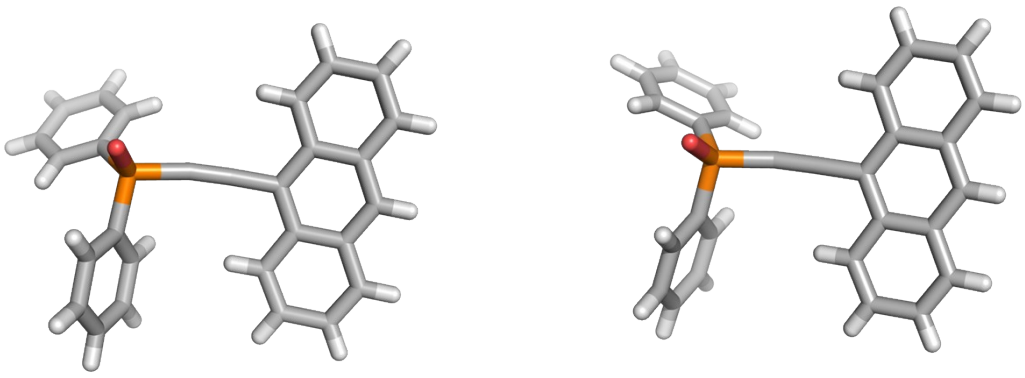

Fig. S30. Crystal structure of [2-(9-anthryl)ethynyl]diphenylphosphine oxide **2a** and **2b** in the stick model (left: **2a**, right: **2b**). Crystal models were created by the PyMOL molecular graphics system. (Gray: C, White: H, Orange: P, Red: O)

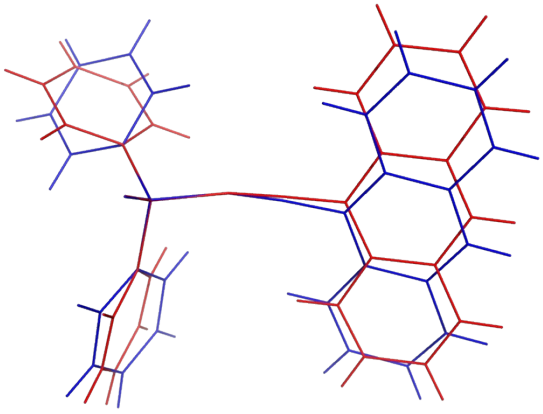

Fig. S31. Overlay of crystal polymorphs **2a** (red) and **2b** (blue).

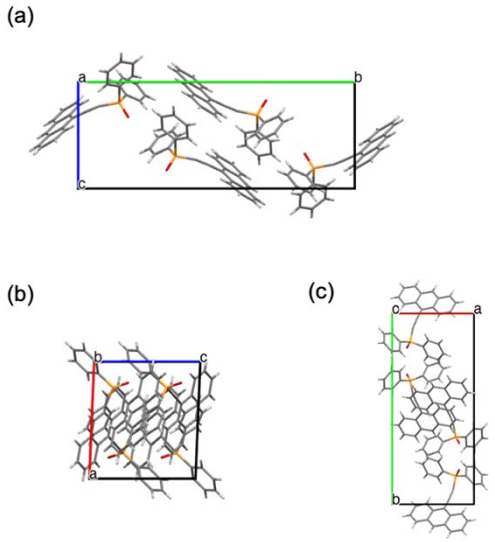


Fig. S32. Crystal packing of **2a** viewed from each direction of *a*, *b*, and *c* axes.

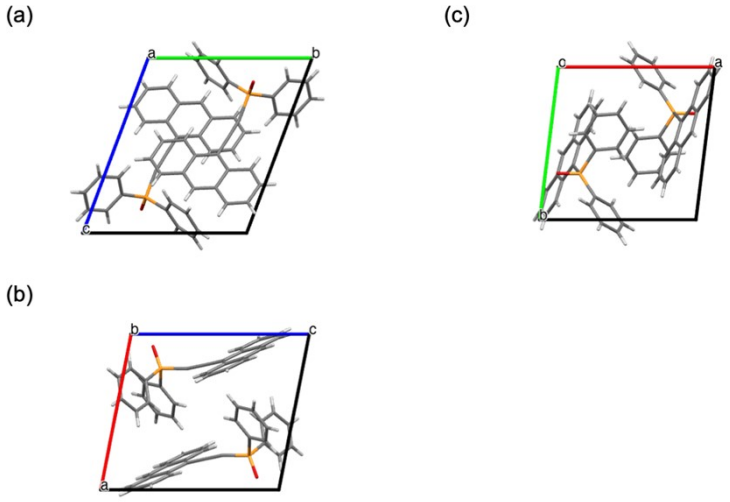


Fig. S33. Crystal packing of **2b** viewed from each direction of *a*, *b*, and *c* axes.

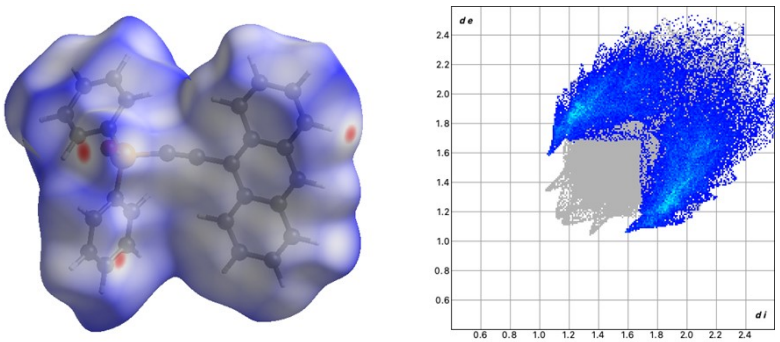


Fig. S34. Selective highlighting of C···H contacts on the Hirshfeld surface of axle of **2a** mapped with $d_{norm}$ surface (left), and fingerprint plots of axle of **2a** resolved into C–H contacts (right). Contribution ratio of the C–H interactions was calculated to be 38.8%. The full fingerprint appears beneath decomposed plots as a gray shadow.

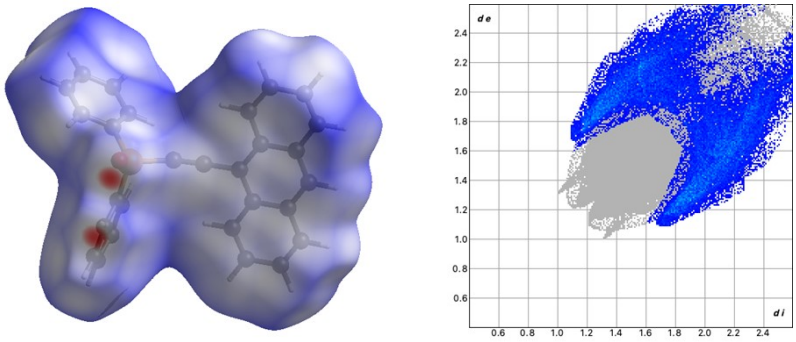


Fig. S35. Selective highlighting of C···H contacts on the Hirshfeld surface of axle of **2b** mapped with $d_{norm}$ surface (left), and fingerprint plots of axle of **2b** resolved into C–H contacts (right). Contribution ratio of the C–H interactions was calculated to be 36.5%. The full fingerprint appears beneath decomposed plots as a gray shadow.

Table S5. Crystal date of [2-(1-pyrenyl)ethynyl]diphenylphosphine oxide **4**

| | **4a** | **4b** |
|---|---|---|
| formula | $C_{30}H_{19}OP$ | $C_{30}H_{19}OP$ |
| formula weight | 426.42 | 426.42 |
| crystal system | monoclinic | monoclinic |
| space group | $P2_1/c$ | $P2_1/c$ |
| a (Å), α (°) | 8.7074(1), 90 | 9.9045(1), 90 |
| b (Å), β (°) | 11.3781(1), 95.787(1) | 19.8613(2), 100.3245(10) |
| c (Å), γ (°) | 21.6228(3), 90 | 11.1604(1), 90 |
| $V$ (Å$^3$) | 2131.33(5) | 2159.88(4) |
| $Z$ | 4 | 4 |
| $R$ | 0.0458, 0.1337 | 0.0395, 0.1068 |
| $D_{calc}$ (gm$^{-3}$) | 1.329 | 1.311 |
| $\mu$ (mm$^{-1}$) | 1.294 | 1.277 |
| GOF | 1.109 | 1.031, |
| $R_1$, $wR_2$ (all data) | 0.0505, 0.1377 | 0.0414, 0.1083 |
| CCDC number | 2432552 | 2432553 |

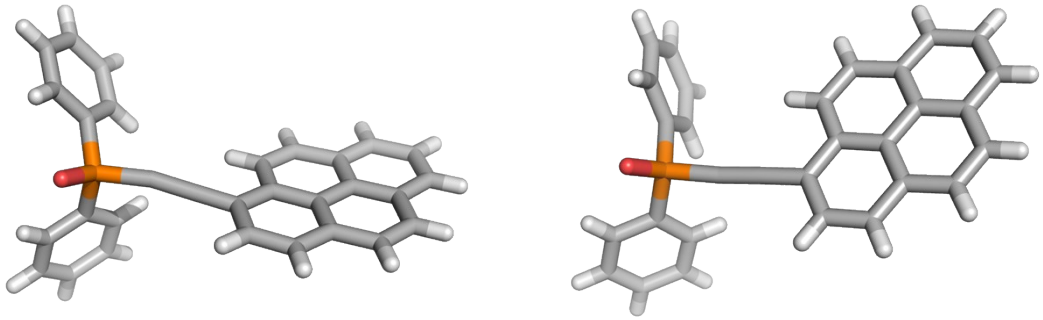

Fig. S36. Crystal structure of [2-(1-pyrenyl)ethynyl]diphenylphosphine oxide **4** in the stick model (left: **4a**, right: **4b**). Crystal models were created by the PyMOL molecular graphics system. (Gray: C, White: H, Orange: P, Red: O)

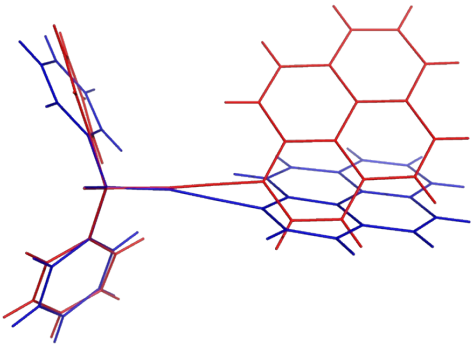

Fig. S37. Overlay of crystal polymorphs **4a** (red) and **4b** (blue).

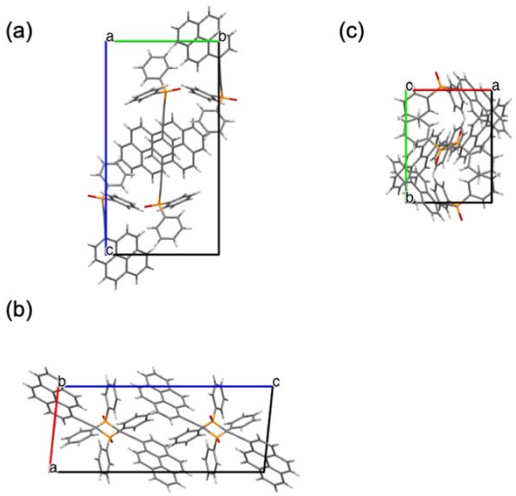

Fig. S38. Crystal packing of **4a** viewed from each direction of *a*, *b*, and *c* axes.

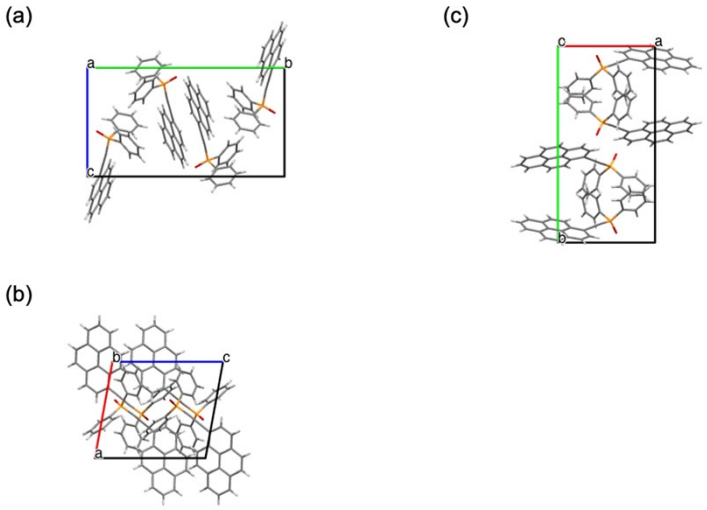


Fig. S39. Crystal packing of **4b** viewed from each direction of *a*, *b*, and *c* axes.

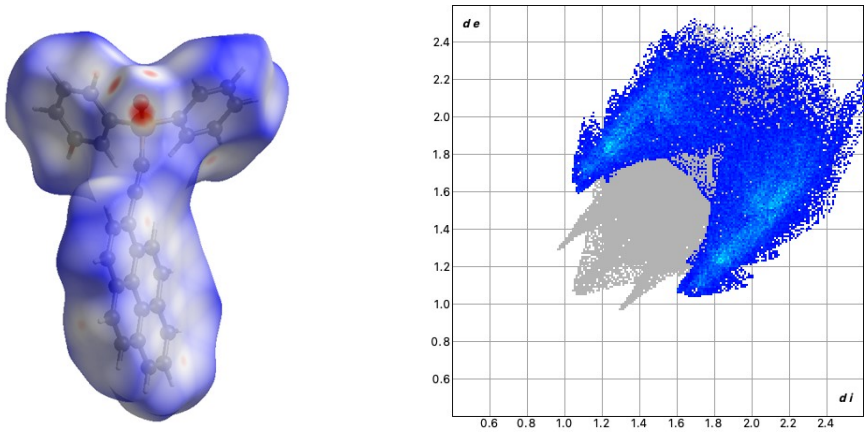


Fig. S40. Selective highlighting of C···H contacts on the Hirshfeld surface of axle of **4a** mapped with $d_{norm}$ surface (left), and fingerprint plots of axle of **4a** resolved into C–H contacts (right). Contribution ratio of the C–H interactions was calculated to be 43.8%. The full fingerprint appears beneath decomposed plots as a gray shadow.

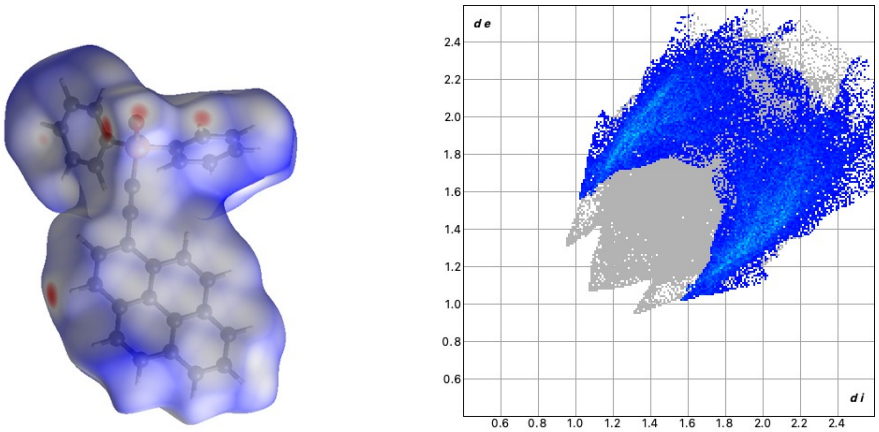


Fig. S41. Selective highlighting of C···H contacts on the Hirshfeld surface of axle of **4b** mapped with $d_{norm}$ surface (left), and fingerprint plots of axle of **4b** resolved into C–H contacts (right). Contribution ratio of the C–H interactions was calculated to be 36.9%. The full fingerprint appears beneath decomposed plots as a gray shadow.

**Powder X-ray Diffraction.** Powder X-ray diffraction patterns were recorded on a Bruker EMPYREAN diffractometer equipped with a CuKα radiation source ($\lambda$ = 1.54184 Å) operating at 45 kV and 40 mA. The data were collected in the range of $2\theta$ = 5-50° with a step size of 0.02° and a scanning speed of 4°/mm.

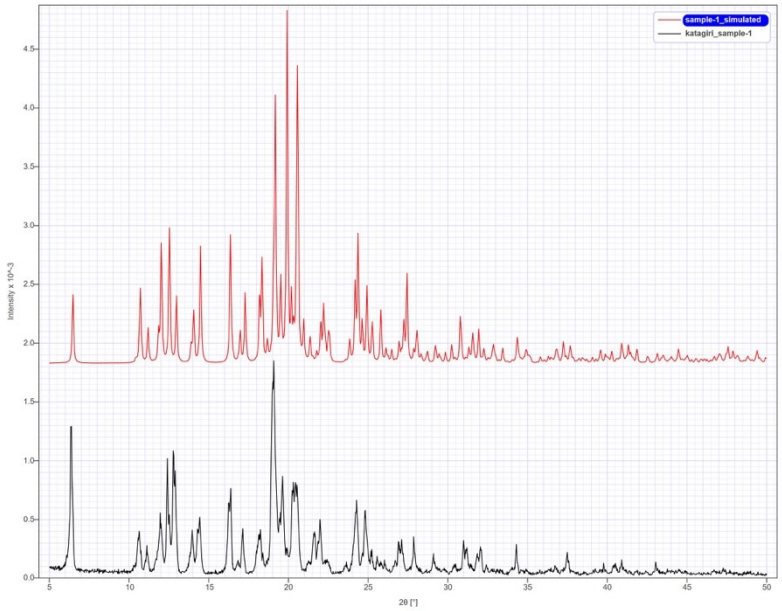


Fig. S42. The PXRD patterns (black line) and simulated data (red line) of crystal **1**.

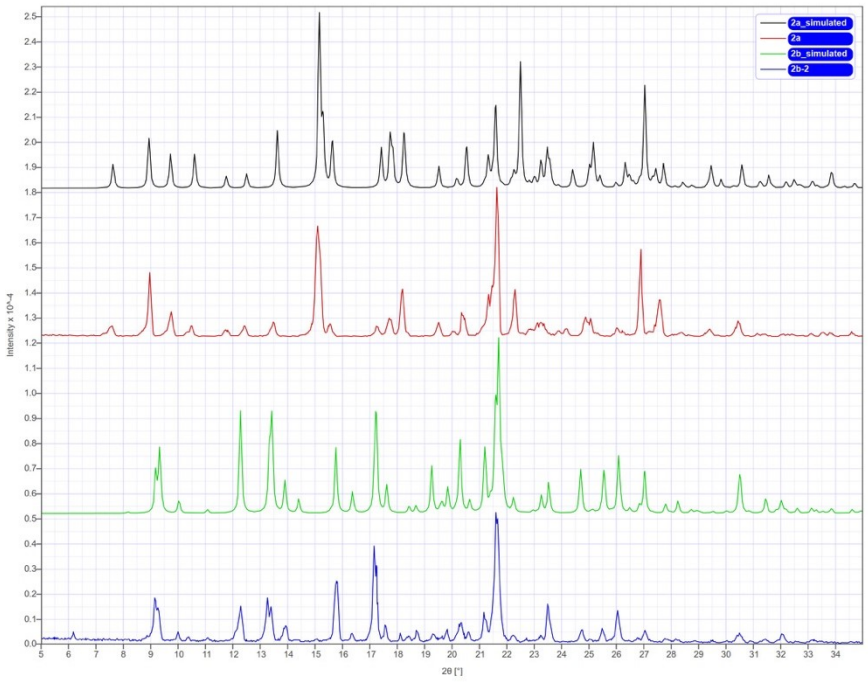


Fig. S43. The PXRD patterns (red line and blue line) and simulated data (black line and

green line) of crystal **2a** and **2b**.

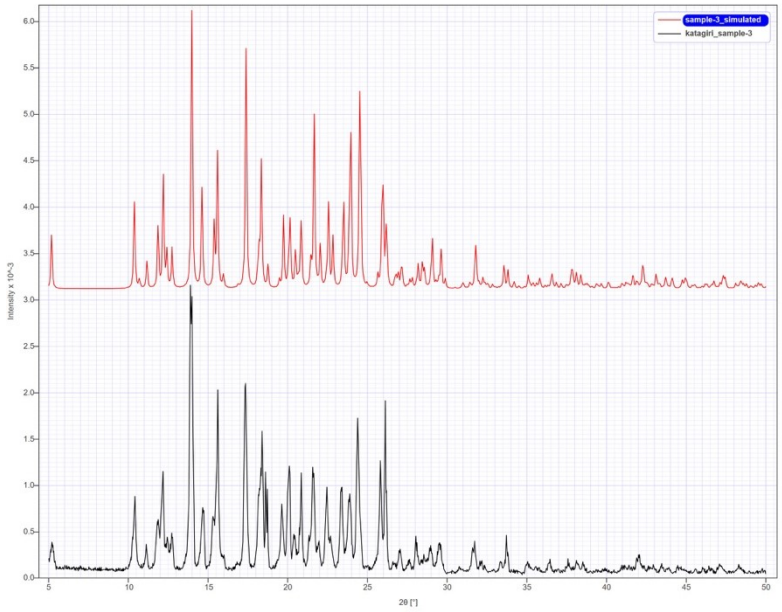


Fig. S44. The PXRD patterns (black line) and simulated data (red line) of crystal **3**.

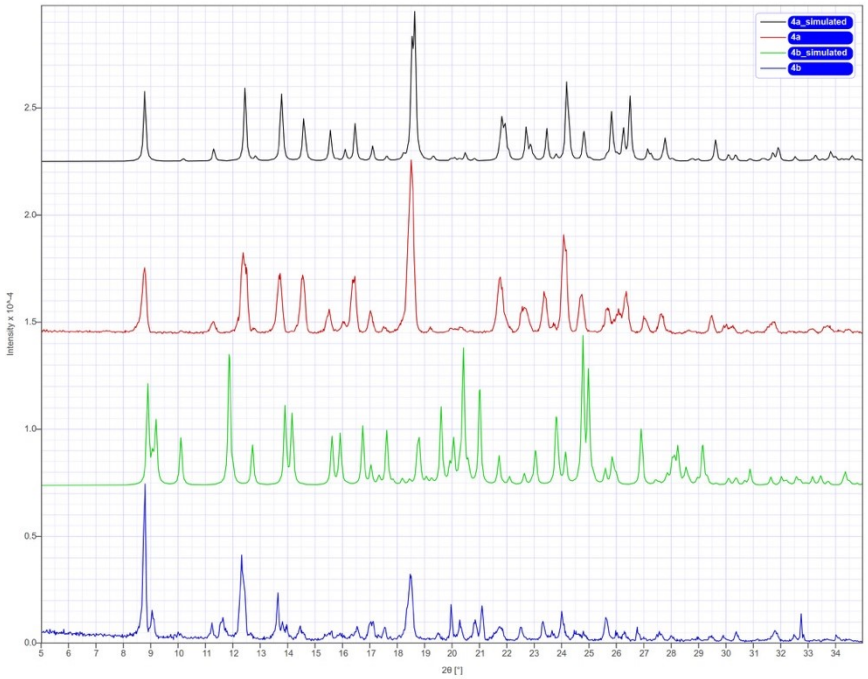


Fig. S45. The PXRD patterns (red line and blue line) and simulated data (black line and green line) of crystal **4a** and **4b**.

**UV-Vis absorption spectra in solution state.**

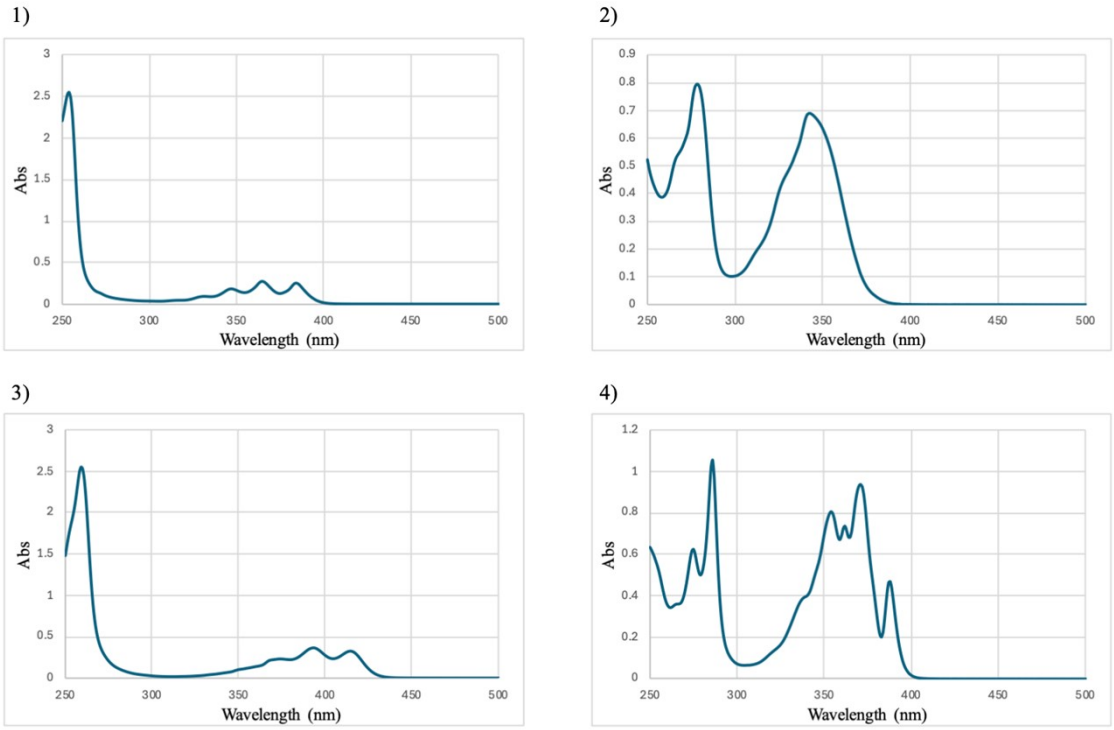


Fig. S46. UV-Vis absorption spectra of 1) [4-(9-Anthryl)phenyl]diphenylphosphine oxide **1**, 2) [4-(1-pyrenyl)phenyl]-diphenylphosphine oxide **3**, 3) [2-(9-anthryl)ethynyl]diphenylphosphine oxide **2**, 4) [2-(1-pyrenyl)ethynyl]diphenylphosphine oxide **4** in $CH_3CN$ (0.1 g/L).

**Fluorescence spectra in solution-state.**

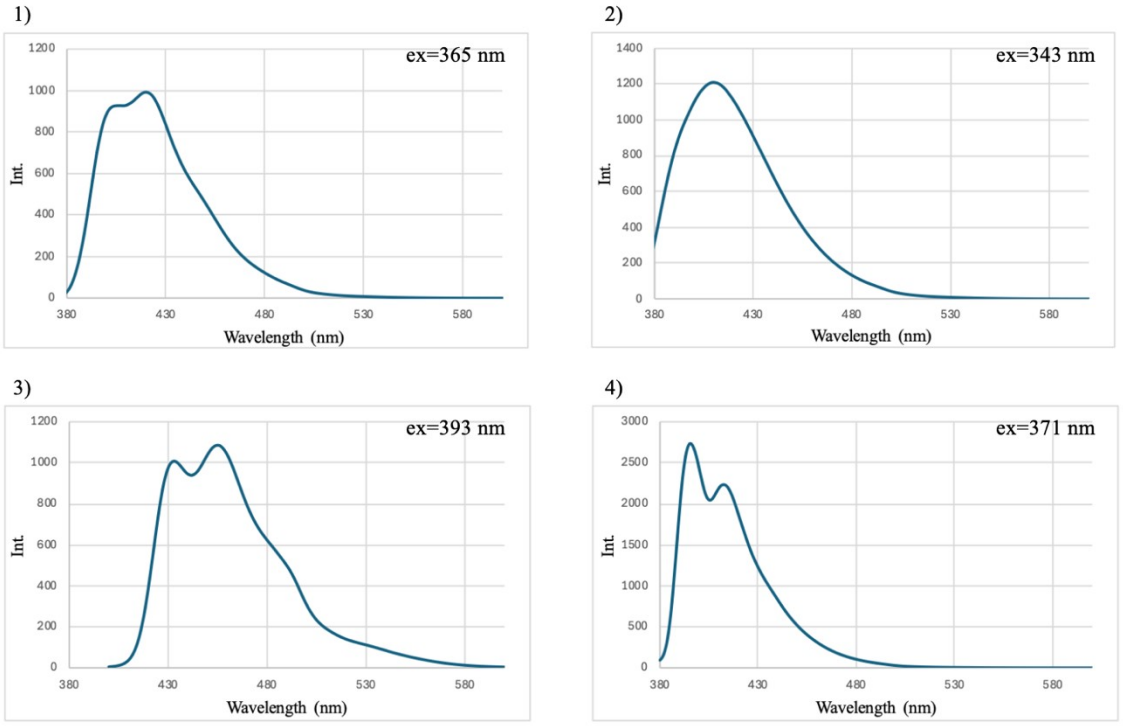


Fig. S47. Fluorescence spectra of 1) [4-(9-Anthryl)phenyl]diphenylphosphine oxide **1**, 2) [4-(1-pyrenyl)phenyl]-diphenylphosphine oxide **3**, 3) [2-(9-anthryl)ethynyl]diphenylphosphine oxide **2**, 4) [2-(1-pyrenyl)ethynyl]diphenylphosphine oxide **4** in $CH_3CN$ (0.1 g/L). "**ex**" is the excitation wavelength.

**UV-Vis absorption spectra in solid state.**

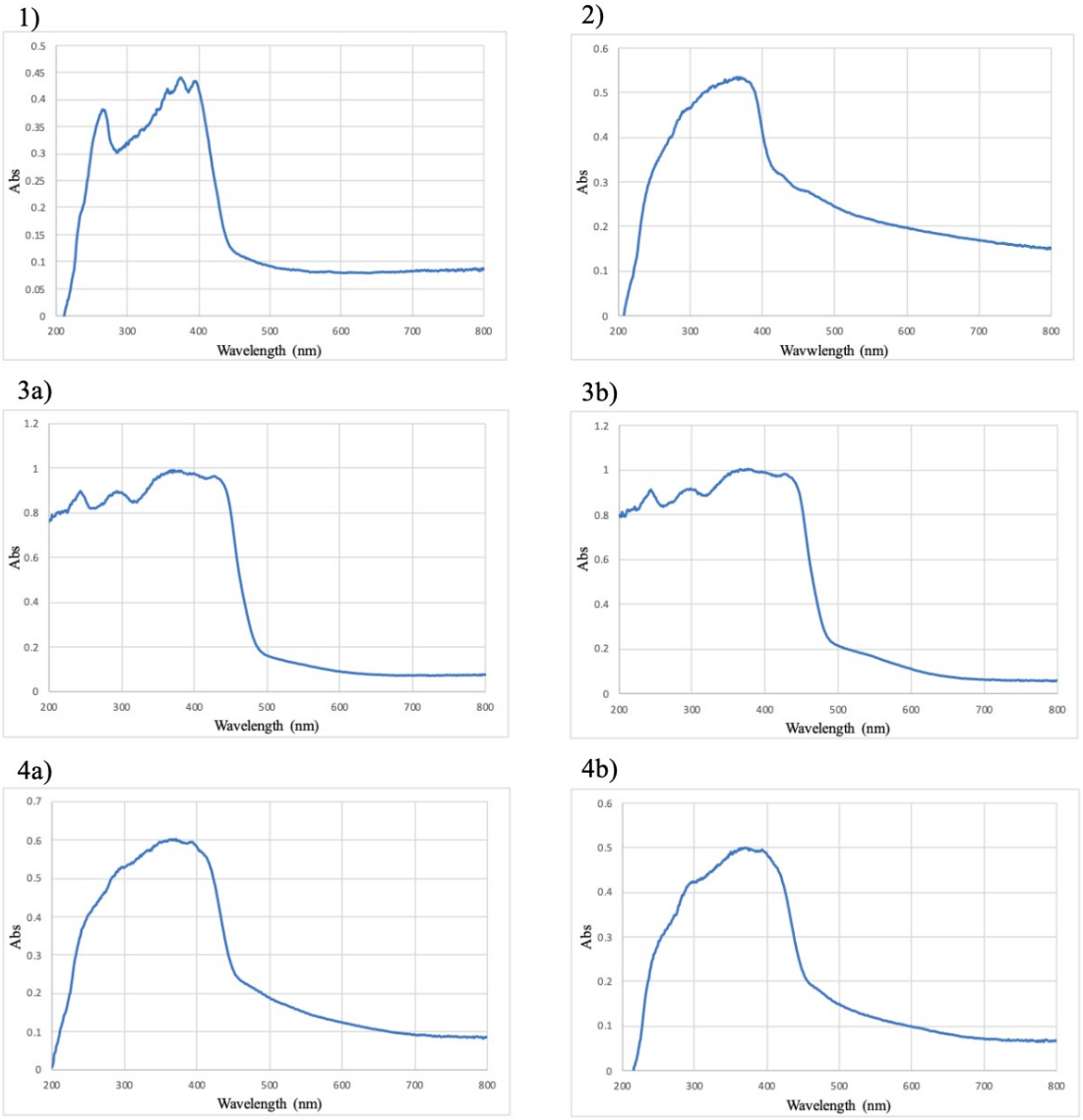


Fig. S48. UV-Vis absorption spectra of 1) [4-(9-Anthryl)phenyl]-diphenylphosphine oxide **1**, 2) [4-(1-pyrenyl)phenyl]diphenylphosphine oxide **3**, 3a) [2-(9-anthryl)ethynyl]diphenylphosphine oxide **2a**, 3b) [2-(9-anthryl)ethynyl]diphenylphosphine oxide **2b**, 4a) [2-(1-pyrenyl)ethynyl]diphenylphosphine oxide **4a**, 4b) [2-(1-pyrenyl)ethynyl]diphenylphosphine oxide **4b** in the solid state.

**Fluorescence Spectra in solid-state.**

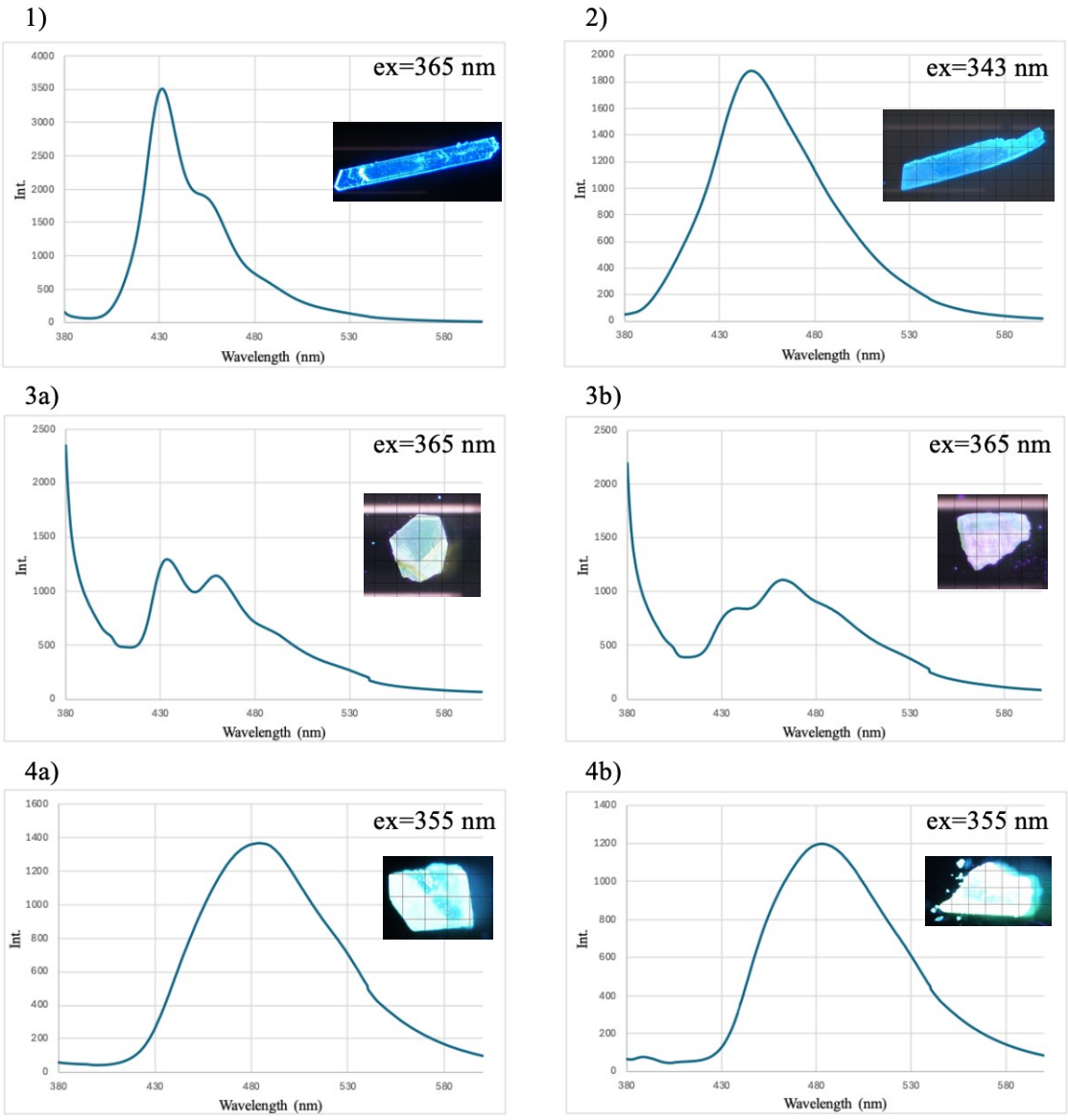


Fig. S49. Fluorescence Spectra of 1) [4-(9-Anthryl)phenyl]diphenyl-phosphine oxide **1**, 2) [4-(1-pyrenyl)phenyl]diphenylphosphine oxide **3**, 3a) [2-(9-anthryl)ethynyl]diphenylphosphine oxide **2a**, 3b) [2-(9-anthryl)ethynyl]diphenylphosphine oxide **2b**, 4a) [2-(1-pyrenyl)ethynyl]diphenylphosphine oxide **4a**, and 4b) [2-(1-pyrenyl)ethynyl]diphenylphosphine oxide **4b** in the solid state. "**ex**" is the excitation wavelength.

**Photoluminescent Quantum Yields (PLQYs) in solid-state.**

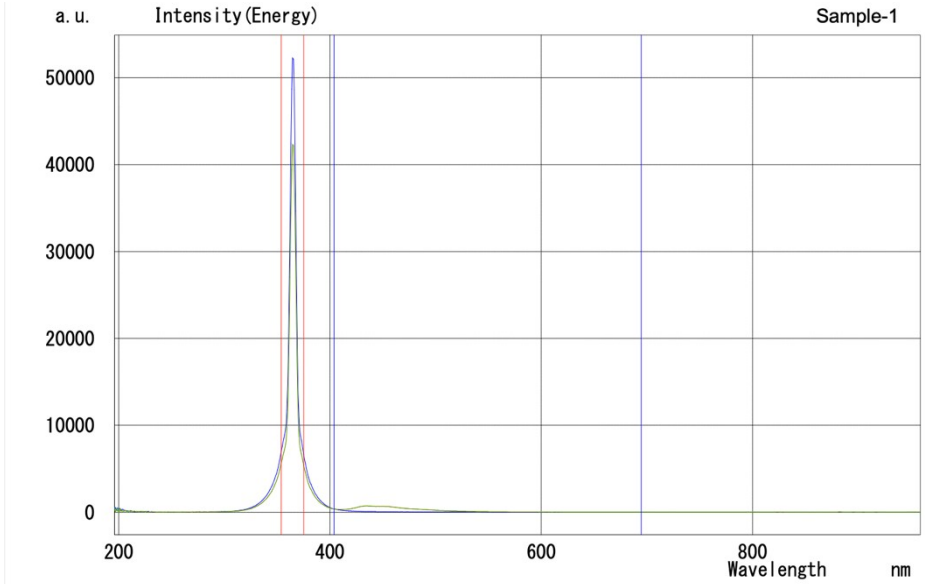


| No. | Cursor1-2: 353.87 – 375.09(nm) | Cursor3-4: 403.83 – 694.66(nm) | QuantumYield | Abs | Peak Wavelength | Peak Count | Peak FWHM | Peak Wavelength | Peak Count | Peak FWHM |
|---|---|---|---|---|---|---|---|---|---|---|
| 1 | 167997397 | ---- | ---- | ---- | 364.48 | 52287.90 | 6.97 | 403.83 | 369.05 | 101.29 |
| 2 | 136469559 | 16195516 | 0.514 | 0.188 | 364.48 | 42201.61 | 7.04 | 434.02 | 721.46 | 62.90 |
| 3 | 136565926 | 16167295 | 0.514 | 0.187 | 364.48 | 42340.61 | 7.02 | 435.53 | 720.07 | 63.15 |

Fig. S50 PQLY of [4-(9-Anthryl)phenyl]diphenyl-phosphine oxide **1**.

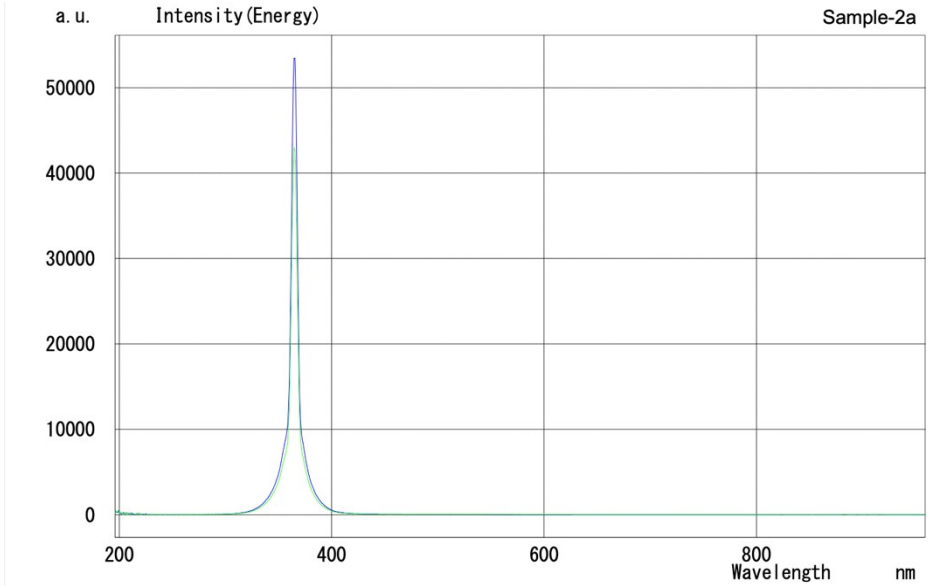


| No. | Cursor1-2: 353.87 – 375.09(nm) | Cursor3-4: 467.91 – 705.75(nm) | QuantumYield | Abs | Peak Wavelength | Peak Count | Peak FWHM | Peak Wavelength | Peak Count | Peak FWHM |
|---|---|---|---|---|---|---|---|---|---|---|
| 1 | 171767678 | ---- | ---- | ---- | 364.48 | 53466.49 | 6.96 | 471.67 | 47.08 | 276.98 |
| 2 | 138603512 | 2229117 | 0.067 | 0.193 | 364.48 | 43002.27 | 7.02 | 512.21 | 71.57 | 122.32 |

Fig. S51. PQLY of [2-(9-anthryl)ethynyl]diphenylphosphine oxide **2a**.

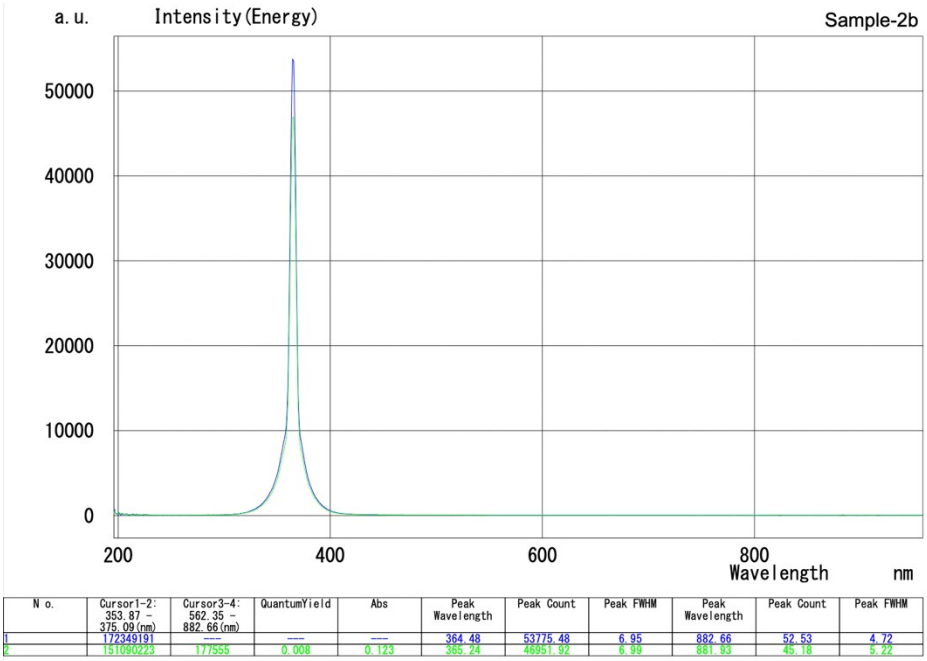


| No. | Cursor1-2: 353.87 - 375.09(nm) | Cursor3-4: 562.35 - 882.66(nm) | QuantumYield | Abs | Peak Wavelength | Peak Count | Peak FWHM | Peak Wavelength | Peak Count | Peak FWHM |
|---|---|---|---|---|---|---|---|---|---|---|
| 1 | 17234191 | --- | --- | --- | 364.48 | 53775.48 | 6.95 | 882.66 | 52.53 | 4.72 |
| 2 | 151090223 | 177555 | 0.008 | 0.123 | 365.24 | 46951.92 | 6.99 | 881.93 | 45.18 | 5.22 |

Fig. S52. PQLY of [2-(9-anthryl)ethynyl]diphenylphosphine oxide **2b**.

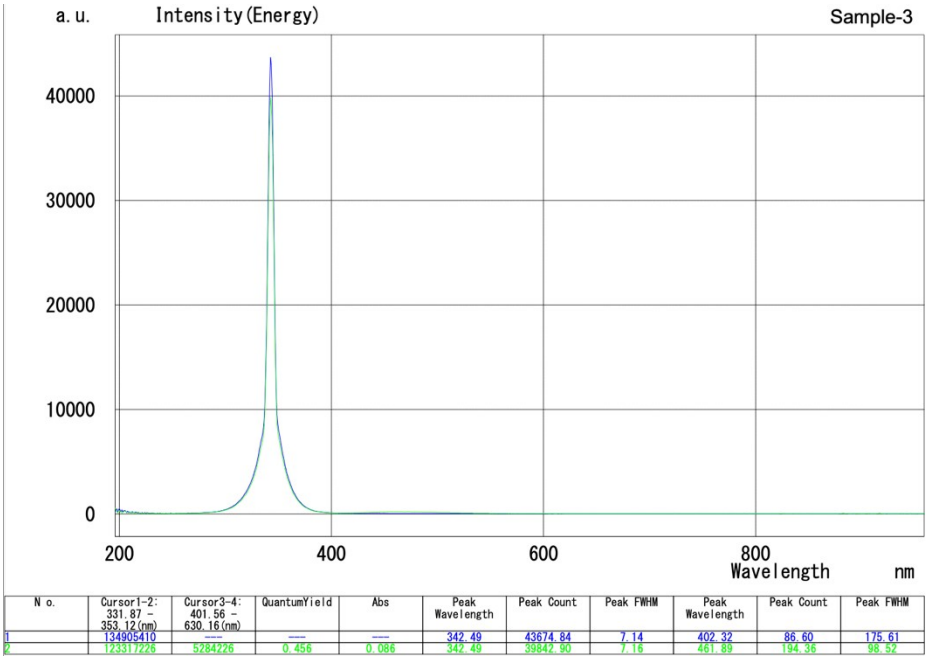


| No. | Cursor1-2: 331.87 - 353.12(nm) | Cursor3-4: 401.56 - 630.16(nm) | QuantumYield | Abs | Peak Wavelength | Peak Count | Peak FWHM | Peak Wavelength | Peak Count | Peak FWHM |
|---|---|---|---|---|---|---|---|---|---|---|
| 1 | 134905410 | --- | --- | --- | 342.49 | 43674.84 | 7.14 | 402.32 | 86.60 | 175.61 |
| 2 | 123317226 | 5284226 | 0.456 | 0.086 | 342.49 | 39842.90 | 7.16 | 461.89 | 194.36 | 98.52 |

Fig. S53. PQLY of [4-(1-pyrenyl)phenyl]diphenylphosphine oxide **3**.

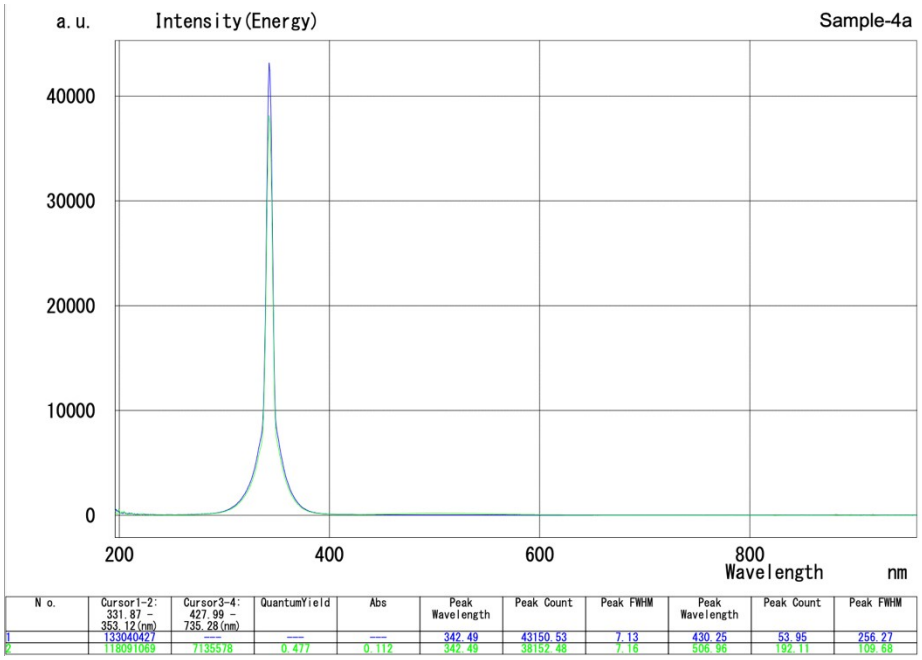


| No. | Cursor1-2: 331.87 - 353.12(nm) | Cursor3-4: 427.99 - 735.28(nm) | QuantumYield | Abs | Peak Wavelength | Peak Count | Peak FWHM | Peak Wavelength | Peak Count | Peak FWHM |
|---|---|---|---|---|---|---|---|---|---|---|
| 1 | 13304027 | --- | --- | --- | 342.49 | 43150.53 | 7.13 | 430.25 | 53.95 | 256.27 |
| 2 | 11809069 | 7135578 | 0.477 | 0.112 | 342.49 | 38152.48 | 7.16 | 506.96 | 192.11 | 109.68 |

Fig. S54. PQLY of [2-(1-pyrenyl)ethynyl]diphenylphosphine oxide **4a**.

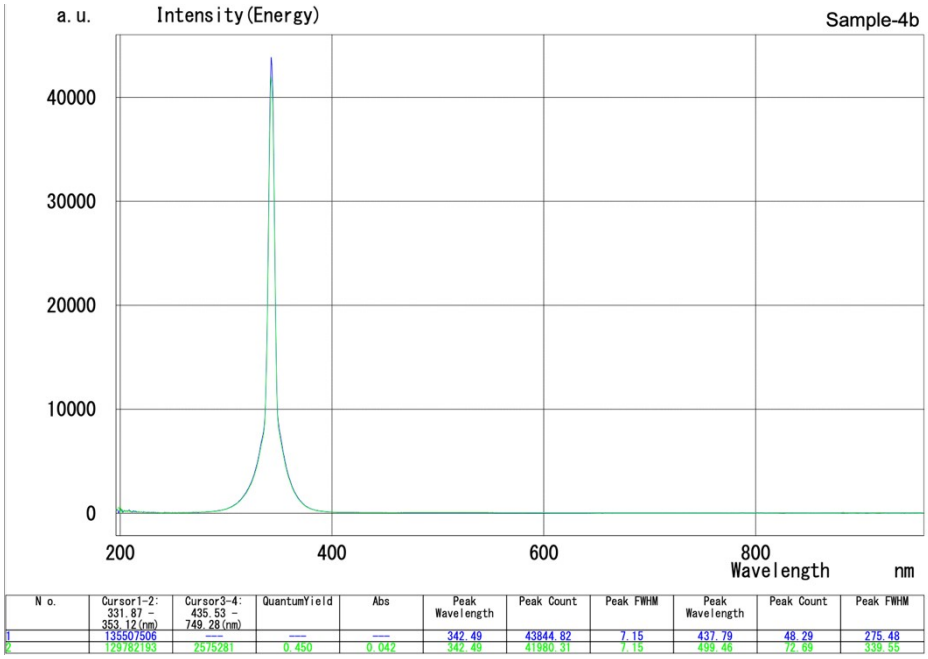


| No. | Cursor1-2: 331.87 - 353.12(nm) | Cursor3-4: 435.53 - 749.28(nm) | QuantumYield | Abs | Peak Wavelength | Peak Count | Peak FWHM | Peak Wavelength | Peak Count | Peak FWHM |
|---|---|---|---|---|---|---|---|---|---|---|
| 1 | 135507506 | --- | --- | --- | 342.49 | 43844.82 | 7.15 | 437.79 | 48.29 | 275.48 |
| 2 | 129782193 | 2575281 | 0.450 | 0.042 | 342.49 | 41980.31 | 7.15 | 499.46 | 72.69 | 339.55 |

Fig. S55. PQLY of [2-(1-pyrenyl)ethynyl]diphenylphosphine oxide **4b**.

**Theoretical Calculation Methods.**

The theoretical calculations of compound **1**, **2a**, **2b**, **3**, **4a** and **4b** were executed by the Gaussian 09 software packcage.[4] The ground state geometry optimizations based on time-dependent density functional theory (TD-DFT)[5] were performed with B3LYP functional[6] and 6-31g(d) basis set.[7]

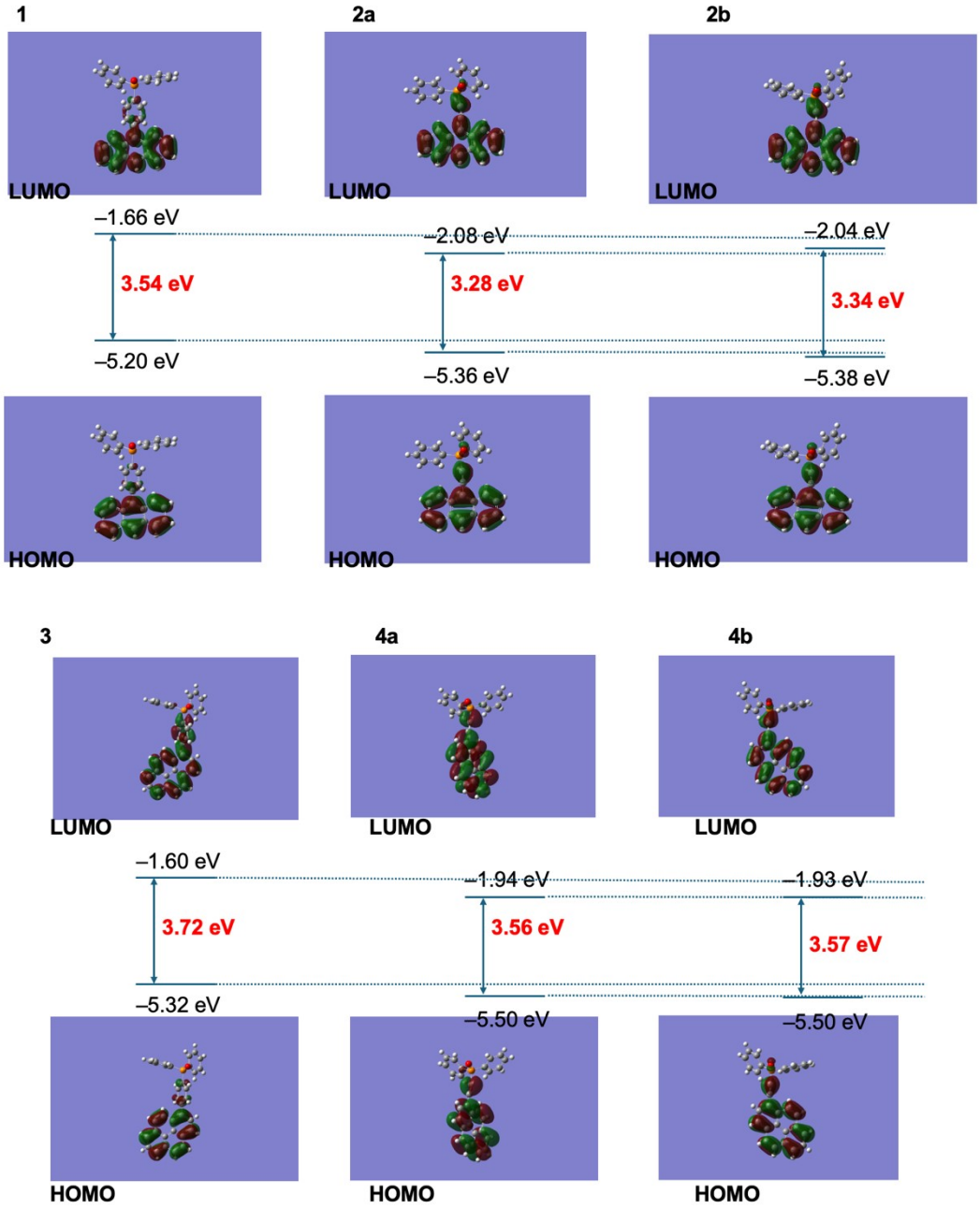


Fig. S56. Theoretical calculations. Frontier-orbital (HOMO/LUMO) distributions, energy levels and energy gaps characterized TD-DFT calculations.

Table S6. Dihedral angles and Torsion angles.

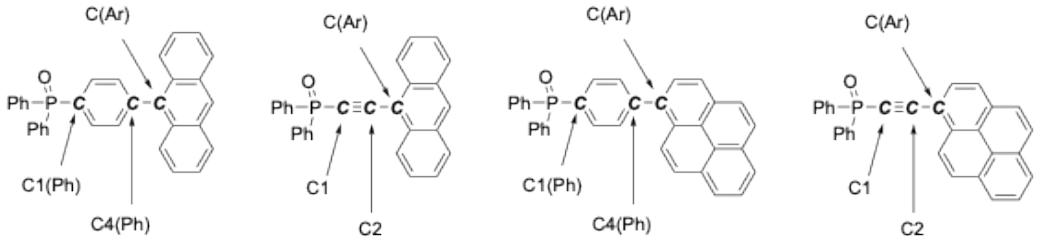


| Crystal | Space Group | ∠P-C1(Ph)-C4(Ph)<br>∠P-C1-C2 | ∠C(Ph)-C4(Ph)-C(Ar)<br>∠C1-C2-C(Ar) | Dihedral angle | Torsion angle<br>∠O_P_C_C |
|---|---|---|---|---|---|
| **1** | $P2_1/n$ | 175.93 ° | 176.31 ° | 71.62 °<br>–108.28° | 104.44 °<br>–73.50 ° |
| **2a** | $P2_1/c$ | 164.50 ° | 175.99 ° | — | 116.95 °<br>–50.54 ° |
| **2b** | $P$-1 | 165.94 ° | 178.34 ° | — | 107.14 °<br>–62.59 ° |
| **3** | $P2_1/c$ | 176.62 ° | 176.54 ° | 128.53 °<br>–55.03 ° | 126.96 °<br>–57.87° |
| **4a** | $P2_1/c$ | 169.22 ° | 179.09 ° | — | –162.68 °<br>–19.01 ° |
| **4b** | $P2_1/c$ | 174.50 ° | 178.88 ° | — | –113.91 °<br>65.46 ° |

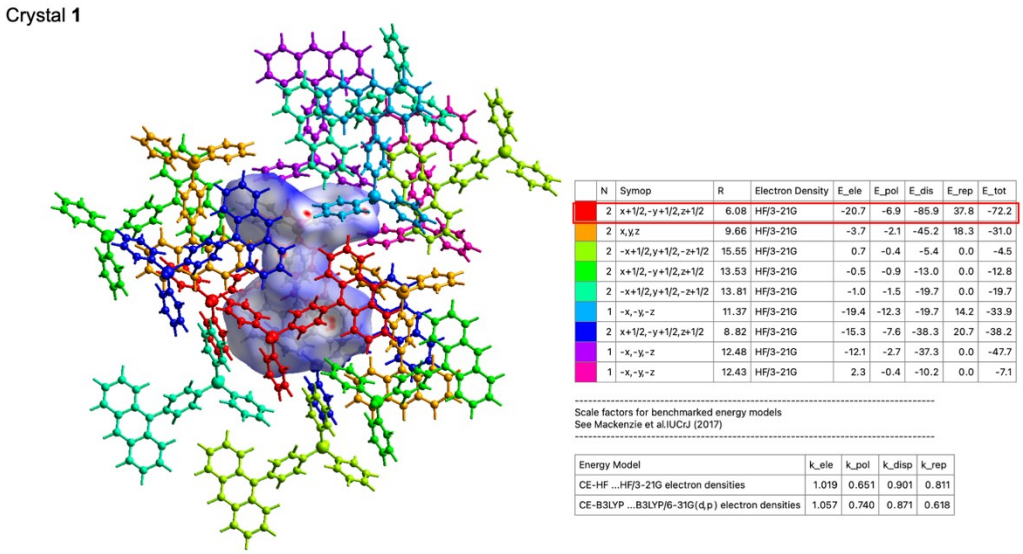


Fig. S57. Interactions with surrounding molecules. The molecular coloring corresponds to the colors in the leftmost column of the table. The values in the first row represent the

energy partition calculations between the central molecule enclosed by the Hirschfeld surface and the red molecules. Energy units in the table are kJ/mol.

Crystal **2a**

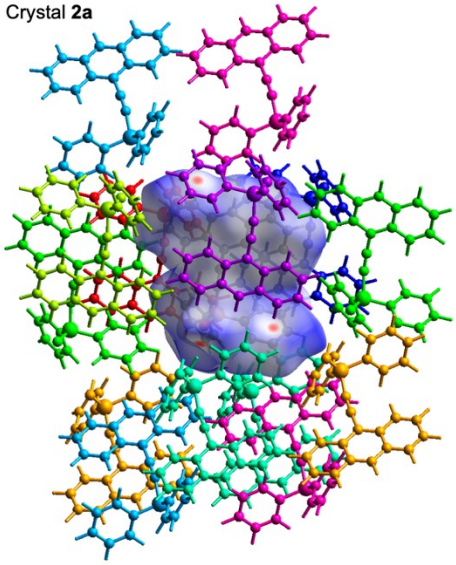

| | N | Symop | R | Electron Density | E_ele | E_pol | E_dis | E_rep | E_tot |
|---|---|---|---|---|---|---|---|---|---|
| | 1 | -x,-y,-z | 7.87 | HF/3-21G | -12.5 | -3.1 | -51.3 | 30.4 | -36.4 |
| | 2 | x,-y+1/2,z+1/2 | 13.94 | HF/3-21G | 4.0 | -0.4 | -3.9 | 0.0 | 0.3 |
| | 1 | -x,-y,-z | 8.72 | HF/3-21G | -21.1 | -13.6 | -44.9 | 24.9 | -50.6 |
| | 2 | x,y,z | 9.89 | HF/3-21G | -0.3 | -2.1 | -27.8 | 13.4 | -15.8 |
| | 2 | x,-y+1/2,z+1/2 | 10.01 | HF/3-21G | -12.0 | -10.4 | -25.7 | 13.0 | -31.6 |
| | 2 | -x,y+1/2,-z+1/2 | 13.27 | HF/3-21G | 4.4 | -0.5 | -5.1 | 0.0 | -0.4 |
| | 1 | -x,-y,-z | 5.95 | HF/3-21G | -23.0 | -5.7 | -79.3 | 36.4 | -69.1 |
| | 1 | -x,-y,-z | 6.50 | HF/3-21G | -33.5 | -13.5 | -123.1 | 71.6 | -95.8 |
| | 2 | -x,y+1/2,-z+1/2 | 12.08 | HF/3-21G | -14.8 | -1.3 | -18.6 | 0.0 | -32.7 |

Scale factors for benchmarked energy models
See Mackenzie et al.IUCrJ (2017)

| Energy Model | k_ele | k_pol | k_disp | k_rep |
|---|---|---|---|---|
| CE-HF ...HF/3-21G electron densities | 1.019 | 0.651 | 0.901 | 0.811 |
| CE-B3LYP ...B3LYP/6-31G(d,p) electron densities | 1.057 | 0.740 | 0.871 | 0.618 |

Fig. S58. Interactions with surrounding molecules. The molecular coloring corresponds to the colors in the leftmost column of the table. The values in the first row represent the energy partition calculations between the central molecule enclosed by the Hirschfeld surface and the red molecules. Energy units in the table are kJ/mol.

Crystal **2b**

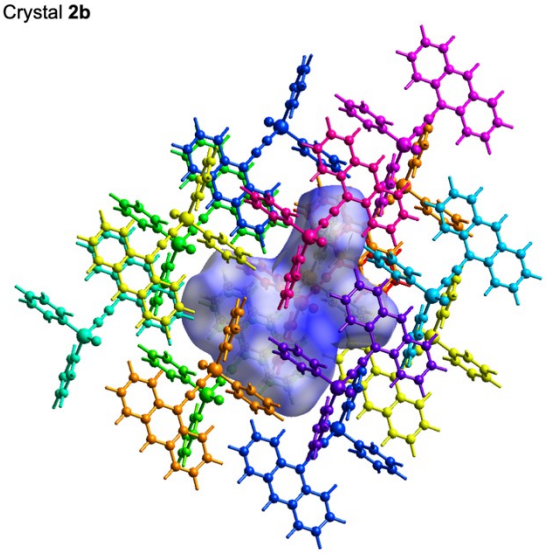

| | N | Symop | R | Electron Density | E_ele | E_pol | E_dis | E_rep | E_tot |
|---|---|---|---|---|---|---|---|---|---|
| | 1 | -x,-y,-z | 8.96 | HF/3-21G | -27.2 | -17.1 | -16.6 | 14.4 | -42.2 |
| | 2 | x,y,z | 11.70 | HF/3-21G | -7.6 | -2.7 | -20.7 | 7.7 | -21.9 |
| | 2 | x,y,z | 12.66 | HF/3-21G | -4.1 | -0.4 | -6.4 | 0.0 | -10.2 |
| | 1 | -x,-y,-z | 6.85 | HF/3-21G | -21.4 | -11.1 | -97.8 | 41.4 | -83.6 |
| | 1 | -x,-y,-z | 8.58 | HF/3-21G | -15.1 | -9.3 | -33.3 | 16.0 | -38.5 |
| | 1 | -x,-y,-z | 15.32 | HF/3-21G | -3.5 | -0.6 | -9.0 | 0.0 | -12.1 |
| | 1 | -x,-y,-z | 10.76 | HF/3-21G | -8.5 | -3.1 | -42.4 | 20.9 | -31.9 |
| | 2 | x,y,z | 10.12 | HF/3-21G | -1.3 | -1.7 | -26.8 | 12.7 | -16.3 |
| | 1 | -x,-y,-z | 6.76 | HF/3-21G | -9.9 | -3.0 | -46.2 | 15.3 | -41.2 |
| | 1 | -x,-y,-z | 14.47 | HF/3-21G | -1.7 | -0.3 | -6.6 | 0.0 | -7.9 |
| | 1 | -x,-y,-z | 7.77 | HF/3-21G | -9.0 | -2.7 | -44.1 | 17.6 | -36.4 |

Scale factors for benchmarked energy models
See Mackenzie et al.IUCrJ (2017)

| Energy Model | k_ele | k_pol | k_disp | k_rep |
|---|---|---|---|---|
| CE-HF ...HF/3-21G electron densities | 1.019 | 0.651 | 0.901 | 0.811 |
| CE-B3LYP ...B3LYP/6-31G(d,p) electron densities | 1.057 | 0.740 | 0.871 | 0.618 |

Fig. S59. Interactions with surrounding molecules. The molecular coloring corresponds to the colors in the leftmost column of the table. The values in the first row represent the

energy partition calculations between the central molecule enclosed by the Hirschfeld surface and the red molecules. Energy units in the table are kJ/mol.

Crystal **3**

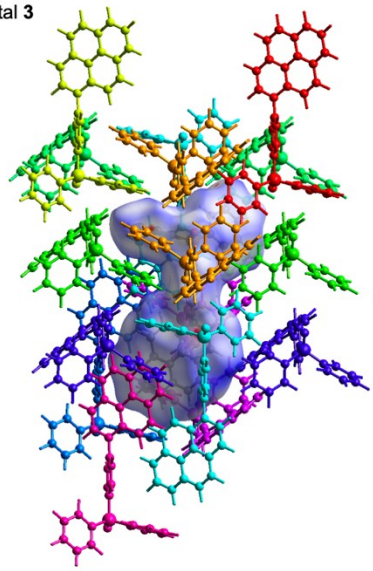

| | N | Symop | R | Electron Density | E_ele | E_pol | E_dis | E_rep | E_tot |
|---|---|---|---|---|---|---|---|---|---|
| | 1 | -x,-y,-z | 14.27 | HF/3-21G | -2.1 | -9.1 | -30.7 | 0.0 | -35.7 |
| | 2 | -x,y+1/2,-z+1/2 | 10.33 | HF/3-21G | -5.8 | -12.4 | -34.7 | 17.6 | -31.0 |
| | 1 | -x,-y,-z | 14.78 | HF/3-21G | -12.1 | -0.8 | -10.3 | 0.0 | -22.2 |
| | 2 | x,-y+1/2,z+1/2 | 8.28 | HF/3-21G | -10.2 | -3.2 | -52.7 | 29.5 | -36.0 |
| | 2 | x,-y+1/2,z+1/2 | 15.15 | HF/3-21G | 0.3 | -0.8 | -13.5 | 0.0 | -12.3 |
| | 2 | x,y,z | 9.45 | HF/3-21G | -13.0 | -3.1 | -46.9 | 22.1 | -39.6 |
| | 1 | -x,-y,-z | 9.33 | HF/3-21G | -9.9 | -2.9 | -56.2 | 29.2 | -39.0 |
| | 2 | x,-y+1/2,z+1/2 | 9.28 | HF/3-21G | -0.0 | -0.9 | -13.4 | 2.2 | -10.8 |
| | 2 | -x,y+1/2,-z+1/2 | 9.49 | HF/3-21G | -12.4 | -3.2 | -42.5 | 19.7 | -37.0 |
| | 1 | -x,-y,-z | 13.93 | HF/3-21G | 70.9 | -5.0 | -54.4 | 0.0 | 20.0 |

Scale factors for benchmarked energy models
See Mackenzie et al.IUCrJ (2017)

| Energy Model | k_ele | k_pol | k_disp | k_rep |
|---|---|---|---|---|
| CE-HF ...HF/3-21G electron densities | 1.019 | 0.651 | 0.901 | 0.811 |
| CE-B3LYP ...B3LYP/6-31G(d,p) electron densities | 1.057 | 0.740 | 0.871 | 0.618 |

Fig. S60. Interactions with surrounding molecules. The molecular coloring corresponds to the colors in the leftmost column of the table. The values in the first row represent the energy partition calculations between the central molecule enclosed by the Hirschfeld surface and the red molecules. Energy units in the table are kJ/mol.

Crystal **4a**

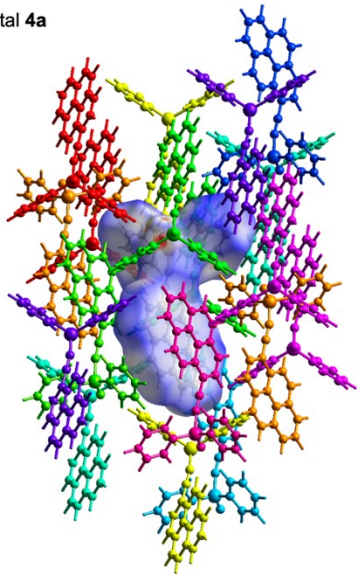

| | N | Symop | R | Electron Density | E_ele | E_pol | E_dis | E_rep | E_tot |
|---|---|---|---|---|---|---|---|---|---|
| | 2 | -x,y+1/2,-z+1/2 | 12.61 | HF/3-21G | -7.0 | -5.9 | -15.3 | 0.0 | -24.8 |
| | 2 | x,y,z | 8.71 | HF/3-21G | 2.8 | -2.2 | -25.8 | 11.9 | -12.2 |
| | 2 | x,-y+1/2,z+1/2 | 13.65 | HF/3-21G | 0.6 | -2.4 | -30.6 | 0.0 | -28.6 |
| | 1 | -x,-y,-z | 7.19 | HF/3-21G | -13.9 | -5.4 | -72.0 | 36.8 | -52.7 |
| | 2 | -x,y+1/2,-z+1/2 | 7.40 | HF/3-21G | -30.1 | -17.3 | -46.7 | 25.9 | -63.0 |
| | 2 | x,-y+1/2,z+1/2 | 11.38 | HF/3-21G | -4.5 | -1.5 | -21.4 | 8.3 | -18.0 |
| | 1 | -x,-y,-z | 12.70 | HF/3-21G | -16.4 | -1.2 | -16.0 | 0.0 | -31.9 |
| | 1 | -x,-y,-z | 15.36 | HF/3-21G | -8.0 | -0.6 | -9.9 | 0.0 | -17.5 |
| | 2 | x,-y+1/2,z+1/2 | 13.34 | HF/3-21G | -1.2 | -0.5 | -3.5 | 0.0 | -4.7 |
| | 2 | -x,y+1/2,-z+1/2 | 10.11 | HF/3-21G | -1.2 | -0.9 | -11.3 | 5.4 | -7.7 |
| | 1 | -x,-y,-z | 8.96 | HF/3-21G | -10.7 | -5.6 | -89.9 | 48.3 | -56.3 |

Scale factors for benchmarked energy models
See Mackenzie et al.IUCrJ (2017)

| Energy Model | k_ele | k_pol | k_disp | k_rep |
|---|---|---|---|---|
| CE-HF ...HF/3-21G electron densities | 1.019 | 0.651 | 0.901 | 0.811 |
| CE-B3LYP ...B3LYP/6-31G(d,p) electron densities | 1.057 | 0.740 | 0.871 | 0.618 |

Fig. S61. Interactions with surrounding molecules. The molecular coloring corresponds to the colors in the leftmost column of the table. The values in the first row represent the

energy partition calculations between the central molecule enclosed by the Hirschfeld surface and the red molecules. Energy units in the table are kJ/mol.

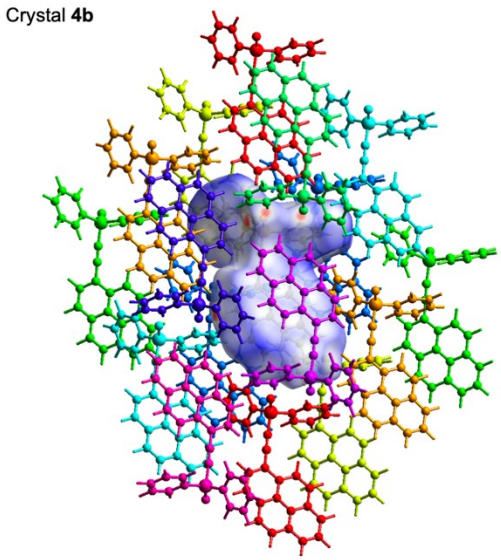


| | N | Symop | R | Electron Density | E_ele | E_pol | E_dis | E_rep | E_tot |
|---|---|---|---|---|---|---|---|---|---|
| | 2 | x,y,z | 13.53 | HF/3-21G | -28.0 | -7.0 | -23.7 | 0.0 | -54.4 |
| | 2 | x,y,z | 9.90 | HF/3-21G | -11.4 | -3.1 | -39.4 | 25.2 | -28.7 |
| | 2 | x,-y+1/2,z+1/2 | 11.68 | HF/3-21G | -2.5 | -2.2 | -32.4 | 15.4 | -20.7 |
| | 2 | x,-y+1/2,z+1/2 | 13.27 | HF/3-21G | 1.2 | -0.2 | -2.5 | 0.0 | -1.1 |
| | 1 | -x,-y,-z | 9.90 | HF/3-21G | -11.1 | -12.6 | -12.2 | 6.4 | -25.3 |
| | 2 | x,y,z | 11.16 | HF/3-21G | -3.7 | -1.0 | -11.9 | 4.7 | -11.4 |
| | 2 | x,-y+1/2,z+1/2 | 7.62 | HF/3-21G | -9.9 | -3.2 | -41.3 | 18.2 | -34.6 |
| | 1 | -x,-y,-z | 7.49 | HF/3-21G | -30.4 | -15.2 | -45.2 | 38.3 | -50.6 |
| | 1 | -x,-y,-z | 7.35 | HF/3-21G | -12.1 | -9.1 | -108.3 | 54.5 | -71.6 |
| | 1 | -x,-y,-z | 14.89 | HF/3-21G | 8.5 | -1.1 | -11.4 | 0.0 | -2.4 |

Scale factors for benchmarked energy models
See Mackenzie et al.IUCrJ (2017)

| Energy Model | k_ele | k_pol | k_disp | k_rep |
|---|---|---|---|---|
| CE-HF ...HF/3-21G electron densities | 1.019 | 0.651 | 0.901 | 0.811 |
| CE-B3LYP ...B3LYP/6-31G(d,p) electron densities | 1.057 | 0.740 | 0.871 | 0.618 |

Fig. S62. Interactions with surrounding molecules. The molecular coloring corresponds to the colors in the leftmost column of the table. The values in the first row represent the energy partition calculations between the central molecule enclosed by the Hirschfeld surface and the red molecules. Energy units in the table are kJ/mol.

## References


1. CrysAlis Pro version 171.39.20a; Rigaku Oxford Diffraction: Tokyo, Japan, 2015.
2. O. V. Dolomanov, L. J. Bourthis, R. J. Gildea, J. A. K. Howard, H. Puschmann, *OLEX2*: a complete structure solution, refinement and analysis program. *J. Appl. Crystallogr.* 2009, **42**, 339–341.
3. (a) G. M. Scheldrick, *Acta Crystallogr. Sect. A: Struct. Chem.* 2008, **64**, 112–122. (b) G. M. Scheldrick, *Acta Crystallogr. Sect. C: Struct. Chem.* 2015, **71**, 3–8.
4. M. J. Frisch, G. W. Trucks, H. B. Schlegel, G. E. Scuseria, M. A. Robb, J. R. Cheesman, Gaussian 09, Revision D.01. Gaussian, Inc., Wallingford CT, (2013).
5. E. Runge, E. K. Gross, Density-Functional Theory for Time-Dependent Systems. *Phys. Rev. Lett.* 1984, **52**, 997–1000.
6. P. J. Stephens, F. J. Devlin, C. F. Chabalowski, M. J. Frisch, Ab Initio Calculation of Vibrational Absorption and Circular Dichroism Spectra Using Density Functional Force Fields. *J. Phys. Chem.* 1994, **98**, 11623–11627.

7. V. A. Rassloov, M. A> Ratner, J. A. Pople, P.C. Redfern, L. A. Curtiss, 6-31G* basis set for third-row atoms. *J. Comput. Chem.* 2001, **22**, 976–984.